ARTICLE

Genome Sequencing of Autism-Affected Families Reveals Disruption of Putative Noncoding Regulatory DNA

Tychele N. Turner,[1] Fereydoun Hormozdiari,[1] Michael H. Duyzend,[1] Sarah A. McClymont,[2] Paul W. Hook,[2] Ivan Iossifov,[3,4] Archana Raja,[1,5] Carl Baker,[1] Kendra Hoekzema,[1] Holly A. Stessman,[1] Michael C. Zody,[4] Bradley J. Nelson,[1] John Huddleston,[1,5] Richard Sandstrom,[1] Joshua D. Smith,[1] David Hanna,[1] James M. Swanson,[6] Elaine M. Faustman,[7] Michael J. Bamshad,[1,8] John Stamatoyannopoulos,[1] Deborah A. Nickerson,[1] Andrew S. McCallion,[2] Robert Darnell,[4,5,9] and Evan E. Eichler[1,5,*]

We performed whole-genome sequencing (WGS) of 208 genomes from 53 families affected by simplex autism. For the majority of these families, no copy-number variant (CNV) or candidate de novo gene-disruptive single-nucleotide variant (SNV) had been detected by microarray or whole-exome sequencing (WES). We integrated multiple CNV and SNV analyses and extensive experimental validation to identify additional candidate mutations in eight families. We report that compared to control individuals, probands showed a significant ($p = 0.03$) enrichment of de novo and private disruptive mutations within fetal CNS DNase I hypersensitive sites (i.e., putative regulatory regions). This effect was only observed within 50 kb of genes that have been previously associated with autism risk, including genes where dosage sensitivity has already been established by recurrent disruptive de novo protein-coding mutations (*ARID1B*, *SCN2A*, *NR3C2*, *PRKCA*, and *DSCAM*). In addition, we provide evidence of gene-disruptive CNVs (in *DISC1*, *WNT7A*, *RBFOX1*, and *MBD5*), as well as smaller de novo CNVs and exon-specific SNVs missed by exome sequencing in neurodevelopmental genes (e.g., *CANX*, *SAE1*, and *PIK3CA*). Our results suggest that the detection of smaller, often multiple CNVs affecting putative regulatory elements might help explain additional risk of simplex autism.

Introduction

The underlying genetic etiology of autism (MIM: 209850) has been an area of intense focus and has benefited considerably from advances in sequencing technology. On the basis of twin studies[1,2] and syndromic forms of the disease,[3,4] autism is known to have a genetic component. With the application of exome sequencing and copy-number variation (CNV) microarrays to large collections of individuals with autism, the genetic architecture of autism has become clearer. Rare and, in particular, de novo variants that disrupt the protein-coding portions of genes and large CNVs are now estimated to contribute to 30% of the diagnoses of simplex autism.[5] In addition, another 7% of cases have been attributed to variants in genes with a residual variation intolerance score (RVIS)[6] < 50, private to a family, and inherited from the mother.[7] One strategy for solving the remaining ~60% is to explore the genome for genetic variants of large effect in families who are already known to be negative for any obvious potential causal variation (de novo likely gene-disruptive [LGD] mutations or large CNVs).

Whole-genome sequencing (WGS) is increasingly becoming more affordable,[8] providing access to a more comprehensive spectrum of genetic variation than is available with previous genomic technologies, including exome sequencing, SNP microarrays, and array comparative genomic hybridization (aCGH), especially within noncoding and potentially regulatory[9,10] regions of the genome.[11] Previous publications have suggested that most of the protein-coding sequence is covered sufficiently well by WGS,[8] which actually provides better coverage[12] than WES technology. Early comparisons, however, were limited. A study of individuals with intellectual disability, for example, made a comparison by using different platforms, i.e., exomes generated by SOLiD or genomes sequenced with Complete Genomics technology. The authors reported a dramatic increase in diagnostic yield as high as 42% for individuals who were previously negative for microarray or exome sequencing,[12] although it was difficult to disentangle these differences from sequence and coverage differences. Another study compared both Illumina WES and WGS but was limited to six individuals.[13] Finally, a more recent analysis of exome and genome sequencing provided a comparison of multiple exome and genome platforms but focused only on a subset of clinically relevant genes[14] as opposed to the whole genome.

In the present study, we specifically compared WGS on the Illumina HiSeq X Ten platform to WES on the NimbleGen capture and Illumina sequencing platforms

[1]Department of Genome Sciences, University of Washington School of Medicine, Seattle, WA 98195, USA; [2]McKusick-Nathans Institute of Genetic Medicine, Johns Hopkins University School of Medicine, Baltimore, MD 21205, USA; [3]Cold Spring Harbor Laboratory, Cold Spring Harbor, NY 11724, USA; [4]New York Genome Center, New York, NY 10013, USA; [5]Howard Hughes Medical Institute, University of Washington, Seattle, WA 98195, USA; [6]Department of Pediatrics, University of California, Irvine, CA 92612, USA; [7]Department of Environmental and Occupational Health Sciences, University of Washington, Seattle, WA 98105, USA; [8]Department of Pediatrics, University of Washington School of Medicine, Seattle, WA 98195, USA; [9]Rockefeller University, New York, NY 10065, USA
*Correspondence: eee@gs.washington.edu

http://dx.doi.org/10.1016/j.ajhg.2015.11.023.

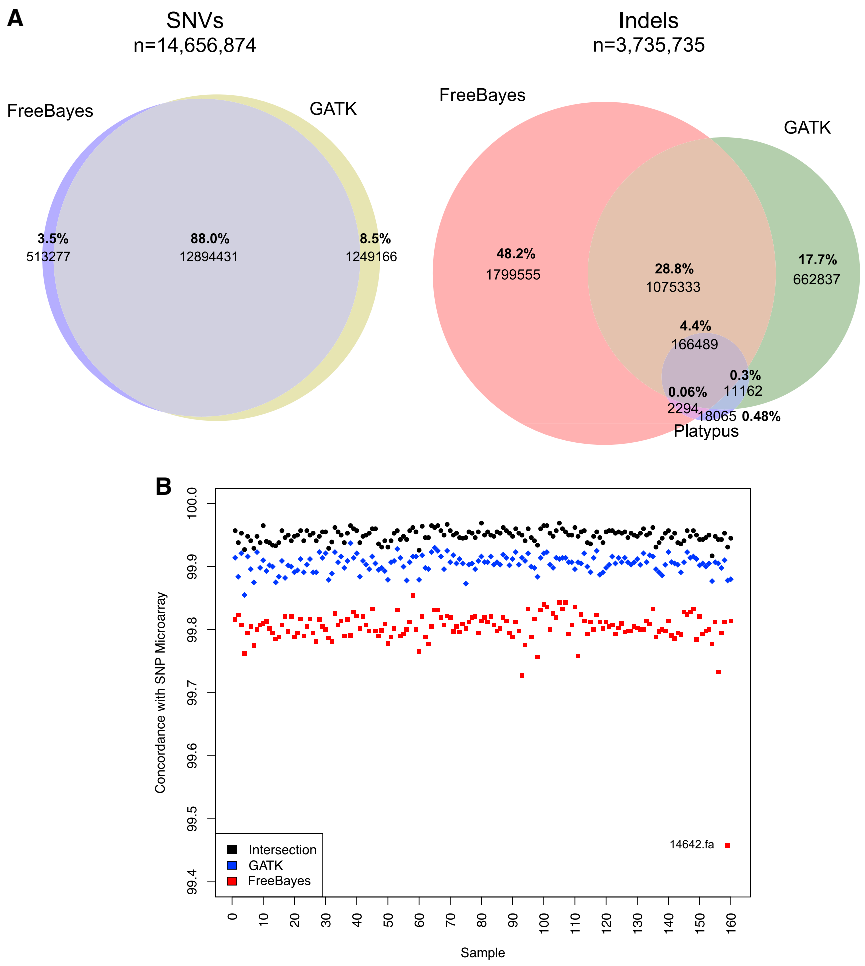

Figure 1. SNV and Indel Analysis

(A) Venn diagram of SNV calls from FreeBayes and GATK and Venn diagram of indel calls from FreeBayes, GATK, and Platypus.

(B) Concordance by sample between variant calls from FreeBayes, GATK, or their intersection (FreeBayes and GATK) and exome-chip data. Variants shown are those passing filters. These data were available for all samples (n = 232,961 variants, of which 44,732 were identified in the genome VCF file). SNP concordance with exome SNP microarrays was 99.80% ± 0.03%, 99.90% ± 0.01%, and 99.95% ± 0.03% for FreeBayes, GATK, and the intersection of FreeBayes and GATK call sets, respectively.

on the same samples. There were two aims. The first was to understand the yield and technological limitations of both WGS and WES approaches in detection of SNVs and CNVs on a sufficiently large sample collection. The second was to assess whether there is any genetic signal for rare and private noncoding regulatory mutations in individuals with idiopathic autism. Using the Illumina HiSeq X Ten platform, we initially focused on 160 individuals from 40 quads with a single proband with autism for which no likely pathogenic CNV or SNV had been originally identified in 39 families (phase I). We performed a follow-up study on another 13 trios with a single autistic proband and three control families by using standard HiSeq 2000 technology (phase II) in order to increase power.

Material and Methods

Phase I families (n = 39) for whom no de novo LGD mutations[5,15–18] or large CNVs[19,20] had been observed in the proband in previous exome and SNP microarray analyses (Figure S1) were selected for WGS from the Simons Simplex Collection (SSC). In addition, one family with a known LGD mutation served as a “control” family for variant detection. We were blinded to this sample initially given that families were selected at the Simons Foundation, and when we detected the event (splice site in *TCF7L2* [MIM: 602228] in proband 13069.p1), we reported to Simons, and they informed us that it was already known. Genomic DNA derived from blood was sequenced to an average depth of 31.1× ± 4.5× (Figure S2A) with an Illumina HiSeq X Ten sequencer at the New York Genome Center (full statistics are shown in Tables S1–S4 and Figure S2). We evaluated the quality of each genome by mapping WGS reads with mrsFAST[21] to the human reference genome (GRCh37, 1000 Genomes), estimating copy number across the entire genome in 500 bp windows (100 bp sliding), and calculating the proportion of known copy-number-invariant regions that were properly called as copy number 2 (diploid) in each genome. The analysis identified four samples (11572.s1, 12175.s1, 12568.s1, and 13023.mo) that did not meet our threshold of >85% “diploidy” (Figure S3A). We used mitochondrial-genome characterization and KING[22] analysis on nuclear genome SNV data to confirm all familial relationships. For the mitochondrial genome, we identified an average of 25 inherited events per family (Tables S5 and S6) and a trend toward excess heteroplasmy in probands (n = 4) rather than siblings (n = 2) (one-sided Fisher’s p = 0.34, odds ratio [OR] = 2.09). We also sequenced 13 trios from the SSC and three control trios from the National Children’s Study (phase II) locally to a median mapped coverage of 51× on an Illumina HiSeq 2000 instrument. Once again, autism trios were selected if they contained no large CNVs according to an aCGH platform[23] or any LGD events revealed through exome sequencing. Between the time the phase II samples were sequenced and this study, it was determined by array that one of these families already contained a known event in *TMLHE* (MIM: 300777) in proband 11000.p1.[24] The institutional review board (IRB) of the University of Washington (IRB 46179) approved this study.

We called SNVs in the phase I genomes by using the Genome Analysis Toolkit v.3.2-2 (GATK best practices) HaplotypeCaller[25,26] and FreeBayes v.0.9.14-20-g5dc4d5e (Figure 1)[27] in addition to Platypus[28] to potentially improve indel sensitivity. Private SNVs and indels were defined as those identified by GATK and FreeBayes (intersection) as having an allele count equal to 1 in parents in this study and not present in dbSNP build 138. De novo SNV and

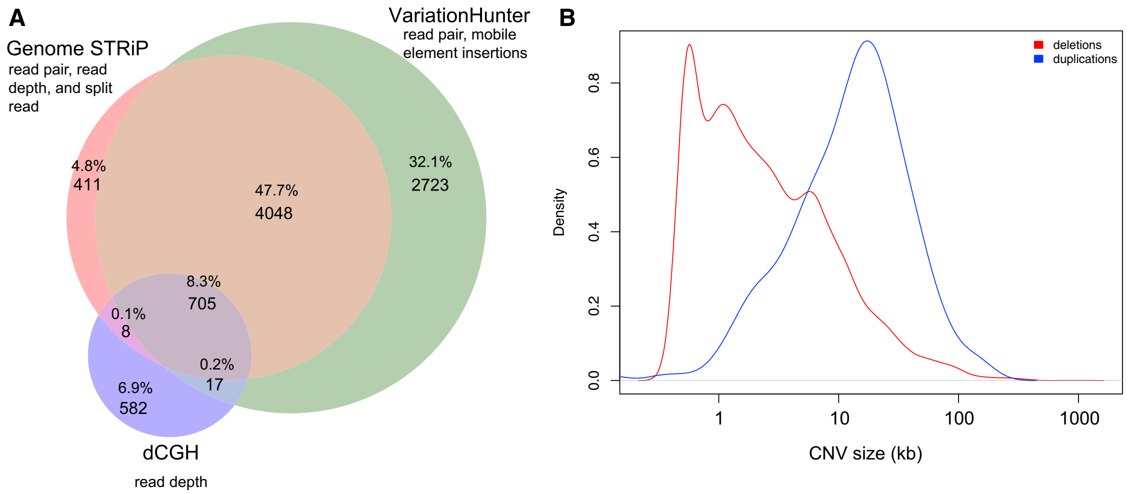

Figure 2. CNV Analysis
(A) Venn diagram of CNV calls from dCGH, GenomeSTRiP, and VariationHunter.
(B) Density of size for deletions and duplications. CNVs were initially merged if they had at least 25% reciprocal overlap and their breakpoints were <1,500 nucleotides away from each other at both ends. To get a very minimal set, we subsequently merged CNVs by using a greedy merge in BEDTools.

indel discovery was achieved with software DNMFilter[29] and TrioDeNovo.[30] In the phase II genomes, reads were mapped with BWA-mem v.0.6.1[31] against GRCh37, and SNVs were called with GATK v.2.7-2 UnifiedGenotyper. Variant quality-score recalibration was applied and excluded tandem repeats, segmental duplications, and dbSNP 129 positions falling in or before release 129. Samples were split into trio variant call format (VCF) files containing entries for mother, father, and proband from each family. Potential de novo SNVs were selected if the alternate allele count in the parents was <2, and a subset of high-confidence SNVs were selected for validation by molecular inversion probe (MIP) resequencing[32] after the call was observed with the Integrated Genomics Viewer.[33] We used ForestDNM[34] on each trio to select putative de novo variants. Variants with a score > 0.7 were considered high-confidence variants and included in the analysis. For de novo indels, we additionally required an allele balance in the proband of 0.25–0.75, no alternate reads present in the parents, and a minimum alternate allele count of 5 in the proband. We used SeattleSeq Annotation 138.8[35] to annotate SNVs and indels.

We called CNVs in phase I genomes by using digital comparative genomic hybridization (dCGH),[36] GenomeSTRiP,[37] and VariationHunter[38] (Figure 2). We merged all CNV calls to a minimal set by combining events with at least 25% reciprocal overlap and breakpoints that were <1,500 nucleotides from each other on both ends. This was applied uniformly to all samples and merged most CNVs, although a few remained unmerged because of separation by segmental duplications or large repeats. For exome-genome comparisons, we used exome calls from XHMM[39] and CoNIFER[40] as described previously.[7] For phase II genomes, CNV calling was limited to VariationHunter (trio-aware CommonLAW)[38] and GenomeSTRiP.[37]

Genic, putative regulatory and repeat-associated variants were annotated with SAVANT.[41] Minor allele frequency was estimated with dbSNP[42] build 138, and a CNV morbidity map was established on the basis of 29,085 case and 19,584 control individuals in whom large (>100 kb) events had been characterized.[43] SNP and CNV genotypes were determined with the Illumina Human Exome 12 v.1.2 exome chip, Illumina whole-genome SNP microarray data,[19] and comparison to exomes (NimbleGen SeqCap EZ Exome Kit v.2 [based on UCSC Genome Browser hg19] and Illumina sequencing) for which BAM and VCF files were available.[7] DNase I hypersensitive sequencing sites were determined on the basis of sequencing of normal human fetal CNS tissues, including 13 brain samples (ages: post-conception days 85–142) and five spinal-cord samples (ages: post-conception days 87–113). After sequencing, the reads were aligned to the human genome, and peaks were called with the Hotspot algorithm[44] using a false-discovery rate (FDR) of 1%. Herein, references to putative regulatory regions refer to these CNS DNase I sites, and putative regulatory variants were considered to be those falling within these regions or with a phyloP score > 4 according to the USCS 46-way alignment. De novo SNVs and indels identified in autistic individuals were collected from the literature[5,7,15–18,32,45] and re-annotated together. Testing for enrichment of de novo events was performed as described previously[32] for LGD, missense, and combined LGD and missense events. A high-confidence set of 57 genes associated with autism risk was generated by the selection of genes with three or more de novo missense and/or LGD events in autistic individuals, one or fewer de novo missense events, and no LGD mutations in control individuals,[5,7] as well as a p value < 0.01 in at least one of the three tests. Enrichment of noncoding putative regulatory regions was tested within regions including and around genes where de novo mutations had been identified. These regions included the transcription start to the transcription stop and extended out from the gene by a given distance (d).

We attempted validation on 691 candidate de novo SNVs and indels in phase I by using Sanger and Pacific Biosciences sequencing. We focused on sites mapping to coding regions and putative, noncoding regulatory elements. In phase II, we used MIP resequencing to validate a subset of putative de novo SNVs and indels.[32] In particular, we made MIP pools for each trio individually and ran mother, father, and proband. Events detected by both GATK and FreeBayes showed the highest validation rate (VR = 89.1%); these were followed by events detected only by GATK (VR = 28.9%) and finally events detected by FreeBayes alone (VR = 10.6%) (Table S7). DNMFilter consistently outperformed

TrioDeNovo for de novo calling within trios. Events called by both DNMFilter and TrioDeNovo had the highest rate (VR = 97.8%), and these were followed by those only called by DNMFilter (VR = 65.5%) and finally events called only by TrioDeNovo (VR = 52.0%) (Table S7). For exonic regions, there were a total of 141 experimentally validated de novo mutations in 80 children. To look at various features important in de novo validation, we performed analysis with random forests[46] and conditional inference trees,[47] similar to the analysis we performed on variants from exome sequencing.[7]

We used two different approaches to validate CNVs. First, we utilized available whole-genome Illumina SNP microarray data and exome-chip data and applied Corrected Robust Linear Model with Maximum Likelihood Classification (CRLMM) software[48,49] to generate probe-level copy-number estimates as described previously.[7] We compared different thresholds on the basis of the number of SNP microarray probes intersecting a CNV ($\geq$5, $\geq$10, or $\geq$20) and assessed ~10% of all CNVs with this approach. Site VRs (whether the site was confirmed in at least one person) were 91.3%, 96.8%, and 97.9% for deletions and 85.6%, 94.4%, and 95.2% for duplications at the $\geq$5, $\geq$10, and $\geq$20 thresholds, respectively. Genotype concordance, however, was significantly reduced at 60.9% ($\geq$5 probes), 67.7% ($\geq$10 probes), and 65.7% ($\geq$20 probes) for deletions, whereas duplications had a genotype concordance of 40.6% ($\geq$5 probes), 49.6% ($\geq$10 probes), and 68.9% ($\geq$20 probes).

In the second approach, we designed a customized microarray (Agilent) for aCGH validation. We targeted 2,002 CNV regions, including all candidate de novo CNVs and all rare, inherited events that had a frequency $\leq$ 4 and that either overlapped an exon or CNS DNase I hypersensitive site or were in a highly conserved region with a maximum phyloP score > 4. The 4×180K Agilent microarray contained 166,175 probes targeting the CNV regions. VRs were very high for events detected by all three callers (98.5%). For unique calls, dCGH showed the highest validation (92.2%) and was followed by GenomeSTRiP (89.1%) and lastly VariationHunter (38.2%). We note that sensitivity ranged by a factor of 3 for these different callers, reflecting the challenge of maintaining a low FDR as part of CNV discovery. Moreover, it is often difficult to validate events < 2 kb in size by aCGH.

We identified 12 CNS DNase I hypersensitive sites within the 14 kb deletion of *DSCAM* (MIM: 602523) in family 11572, and all were selected for functional testing. Nine sequence intervals (150–630 bp), encompassing either one or two of the 12 CNS DNase I hypersensitive sites within the interval, were synthesized as gBlocks (IDT) to be flanked by modified Gateway arms.[50] Sequences separated by $\leq$100 bp were grouped into a common interval for the transgenic assay. The gBlocks were cloned (Gateway LR Clonase) into the pTEA vector, a version of pT2cfosGW[51,52] modified to express the red fluorescent reporter tdTomato, for injection into zebrafish embryos. Zebrafish were maintained as previously described.[53,54] At least 150 embryos were injected per construct at the 1- to 2-cell stage with tol2 transposase RNA as previously described.[51,52] Injected (mosaic) embryos were screened for tdTomato expression at 48 hr post fertilization (hpf). Mosaic embryos were scored positive if they had robust tdTomato CNS expression. The >20% threshold is an empiric cutoff used for determining the likelihood that injected constructs will show that same tissue expression when it is transmitted through the germline. Because all constructs showed CNS expression in >20% embryos, the results are consistent with strong drivers of expression. Embryos were then live imaged at 48 hpf with a Nikon AZ100 Multizoom microscope with NIS-Elements AR 3.2 64 bit software.

Results

SNV and Indel Discovery and Analysis

Applying two SNV and indel callers to WGS data, we identified 1,563,113 private or rare variants detected in the intersection of GATK and FreeBayes in probands and siblings. WGS SNP call sets were high according to a comparison to SNP microarrays (>99%) (Figure 1B). WES call sets showed lower concordance with WGS data (99.08% ± 0.83%) than with SNP microarray genotypes (99.96% ± 0.02%) (Figure S4). Although we observed no significant difference between probands and siblings in terms of overall variant counts (Table S8), probands showed a slight excess of highly conserved missense variants (phyloP > 4) in genes associated with autism risk variants (ten in probands versus seven in siblings). We initially identified 5,609 de novo SNVs and indels by using DNMFilter (70.1 ± 12.0 variants per individual). De novo variants showed evidence of nonrandom clustering (Figure S5), and the number of new mutations significantly correlated with paternal age (Figure 3A) as described previously.[18,55] Application of a second caller, TrioDeNovo, discovered an additional 2,341 variants (missed by DNMFilter), albeit with a lower VR. In total, we detected 7,978 de novo events (7,936 SNVs and 42 indels) and an overall VR of 75.2% for tested variants (Table S7). The most common cause of false positives was under-calling in the parent (which can be approximated by a probability score in DNMFilter; see Figures S6–S10 and, for a full table with features, Table S9).

CNV Discovery and Analysis

We identified a total of 388,538 CNV events corresponding to 9,917 distinct genomic regions in the 160 phase I genomes. Overall, probands showed slightly more (n = 101,257) than siblings (n = 95,727; one-sided paired t test $p = 1.8 \times 10^{-3}$). Leveraging available SNP microarray data for 140 samples, we validated CNVs by using a custom permutation test and CRLMM (see Material and Methods, Figure S11, and Tables S10 and S11). Requiring a minimum of ten SNP microarray probes, we obtained site VRs of 96.8% for deletions and 94.4% for duplications, although genotyping concordance was significantly lower (Material and Methods). To further assess the validation of rare and de novo events, we applied a targeted aCGH approach. We tested 1,529 rare, inherited, and de novo CNVs in all 80 probands and siblings (n = 40 quads) and obtained an overall VR of 91.9% (Table S12). We validated five de novo CNVs in these families (two in probands and three in siblings). The de novo events included an *SAE1* (MIM: 613294) exonic duplication (52 kb) in proband 13874.p1 and a *CANX* (MIM: 114217) promoter and

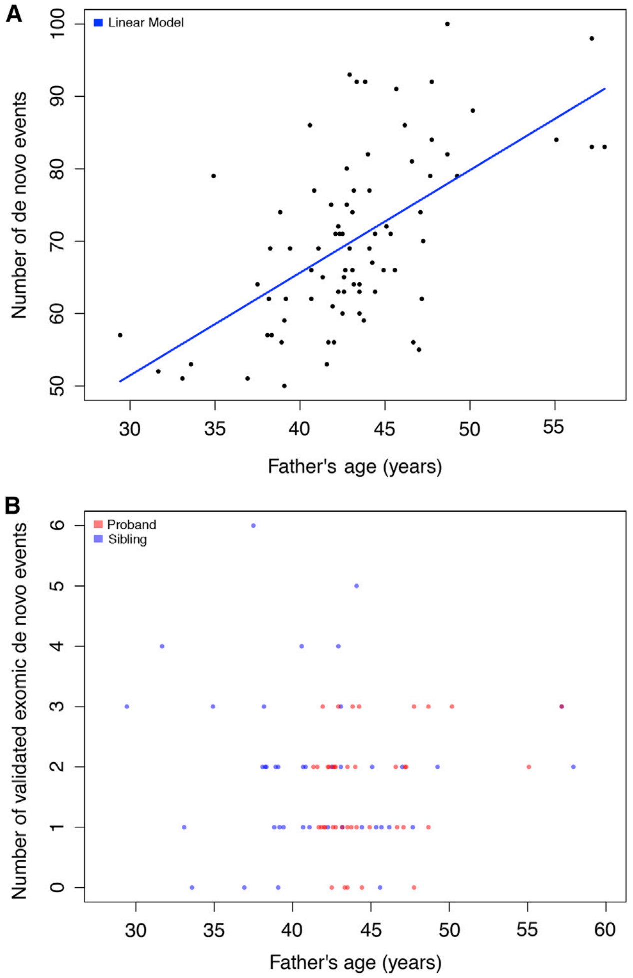

Figure 3. Paternal Age and De Novo Events

(A) Paternal age for de novo SNVs and indels. Probands generally have older fathers. The number of variants was significantly correlated with paternal age (Pearson correlation $p = 7.9 \times 10^{-9}$, $r = 0.59$). The data fit a linear trend (adjusted $r^2 = 0.34$) with advancing paternal age ($p = 7.9 \times 10^{-9}$) such that there are on average 1.4 [0.98, 1.9] de novo mutations for each year of a father's life. In this study, the father's age at the time of the child's birth ranged from 29.4 to 57.9 years.

(B) Paternal age for de novo SNVs and indels within the exome. The number of de novo events detected in each individual is plotted against the father's age when the individual was born. Shown in blue are siblings, and in red are probands.

exon 1 deletion (6 kb) in proband 14153.p1. Sibling de novo events included *ATP2C2* (MIM: 613082) and *TLDC1* deletions (84 kb) in sibling 13874.s1, *PMAIP1* (MIM: 604959) and *MC4R* (MIM: 155541) duplications (1.3 Mb) in sibling 13023.s1, and an *EIF5B* (MIM: 606086) deletion (6 kb) in sibling 12175.s1. Restricting our analyses to the 3,193 de novo and private CNVs (which were identified in only one family in our study and had a frequency < 0.1% in 19,584 control individuals) in probands (n = 1,589) and siblings (n = 1,604), we found no significant difference in size, genic content, or transmission bias between siblings and probands, possibly because of the CNV exclusion criteria for probands (Table S13). Considering all genic regions in the human genome, we found no enrichment of noncoding putative regulatory CNV events in probands (n = 417 in probands versus n = 449 in siblings).

Exome versus Genome

Sequence coverage was predictably[13,56] more uniform by WGS (36.6× ± 5.4×) than by WES (81.2× ± 38.6×) (Figure S12). WGS-only regions were higher in GC content (60.4% ± 0.2%, $p < 2.2 \times 10^{-16}$) than were WES-only regions (47.4% ± 0.1%) (Figure 4). WGS recovered 1,854 genes that were missing WES data for >90% of samples, whereas WES detected only two genes (*ATP6V1G3* and *SLCO1B1* [MIM: 604843]) that were missing WGS data in >90% of samples (Figure 5). Consequently, SNV and indel calling within exome targets was also more uniform by WGS (22,464 ± 578) than by WES (22,172 ± 3,207) (Figure 5). In the genome, the variability was primarily driven by ancestry (Figure S3B), and no such effect was seen in the exome calls, which showed rather stochastic variability across samples. Combining the WES and WGS data, we identified 176,131 exonic SNV and indel events. Of these, 53.9% were found by both WES and WGS, 35.2% were detected by WGS, and 10.8% were detected by WES.

In general, WES-specific sites showed higher sequence coverage (Wilcoxon $p < 2.2 \times 10^{-16}$), but examination of the unfiltered VCF files from WGS recovered most of these (93.7%), suggesting that the exclusion was a result of filters applied to the VCF files. Similarly, 78.9% ± 10.5% of WGS-specific sites within exome capture sites could be recovered in the raw exome VCF files (Figure S13). Ultimately, 3.1% and 3.0% of sites were WES and WGS specific, respectively. We combined data from our current study and from previously published exome studies to obtain the most comprehensive set of de novo variants in the protein-coding regions of these samples (Table S14). There were 210 such variants, of which 173 resided within the NimbleGen exome-capture regions. Of these events, 105 (VR = 93.3%, n = 104 tested) were detected by both exome and genome sequencing, 21 (VR = 35.0%, n = 20 tested) were detected by only exome sequencing, and 47 (VR = 37.1%, n = 35 tested) were detected only by genome sequencing. Overall, we estimate 1.8 ± 1.2 validated de novo exonic mutations per child, which is significantly higher than many of the earlier exome reports. These findings highlight the value of combining WGS and WES to maximize SNV sensitivity. However, fully determining the extent will require much larger sample sizes. With respect to CNVs, WES provided no additional gain in sensitivity (Figures S4B and S14). Moreover, events detected by WGS were 3-fold smaller (10 ± 24 kb, median = 2 kb) than those detected by WES analysis (38 ± 64 kb, median = 7 kb; Wilcoxon $p = 1.4 \times 10^{-7}$). Our comparison of CNV calls from WGS and SNP microarrays also indicated detection of additional CNVs by WGS: 6,898 smaller CNVs less than 50 kb were not detected by CNV calling in SNP microarrays (Figure S15).

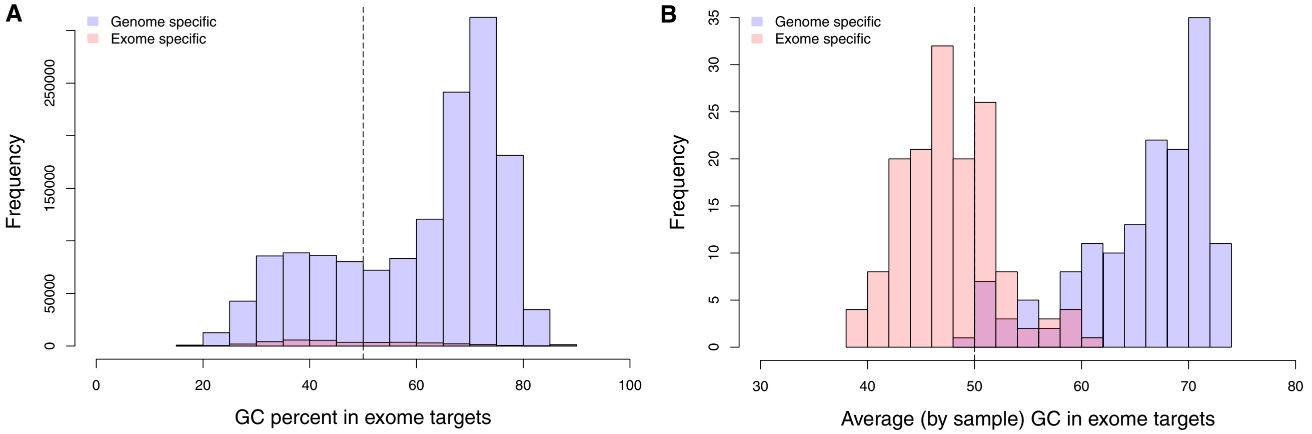

Figure 4. Exome versus Genome: GC Bias
(A) Percentage of GC content in exome-specific sequencing and genome-specific sequencing regions within the exome.
(B) Percentage of average GC content by sample of exome-specific sequencing and genome-specific sequencing regions within the exome. Genome-specific regions are defined as those at >10× coverage in the genome and <10× coverage in the exome. Exome-specific regions are defined as those at >10× coverage in the exome and <10× coverage in the genome. Genome-specific regions are higher in GC content (Wilcoxon $p < 2.2 \times 10^{-16}$).

Smaller CNV and Noncoding Putative Regulatory Mutations in Autism Genomes

In this study, we specifically focused our analysis on noncoding de novo SNVs and indels. In particular, we restricted our analysis to putative regulatory sites, defined as sites in a fetal human CNS DNase I hypersensitive region and/or at a highly conserved base (phyloP score > 4, UCSC 46-way alignment). We attempted Sanger or Pacific Biosciences validation on all such regulatory sites in phase I and combined the validated events with all events identified in the intersection of FreeBayes and GATK (VR = 89.1%) to generate a high-confidence de novo SNV and indel dataset. These data contained 204 noncoding putative regulatory events in probands and 171 in siblings, which did not meet significance (p = 0.07, paired t test) after we accounted for paternal age.

Although it was underpowered, we repeated the analysis by limiting to 57 genes where an excess of recurrent de novo mutations had been identified in probands on the basis of recent exome sequencing studies of families

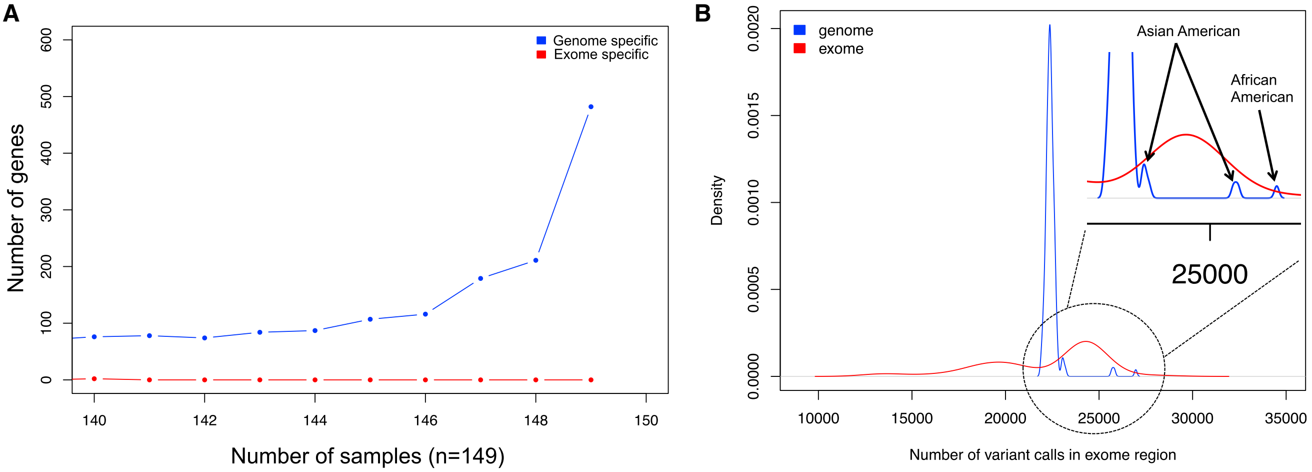

Figure 5. Exome versus Genome: Gene Coverage
(A) Number of genes that have regions covered in exome-specific sequencing or genome-specific sequencing regions of the exome and the number of samples in which they occur. Genome-specific regions of the exome add an additional ~2 Mb (5%) of sequence, whereas exome-specific regions add an additional ~40 kb. Genome sequencing detected 1,854 genes missing sequences in >90% of individuals targeted by exome sequencing, whereas exome sequencing identified only two genes missing sequences in >90% of samples targeted by genome sequencing. Among the genes ascertained only by WGS, those of interest in relation to autism include *ACHE* (MIM: 100740), *AGAP2* (MIM: 605476), *ARID1B*, *CACNA2D3* (MIM: 606399), *DEAF1* (MIM: 602635), *EFR3A* (MIM: 611798), *FOXP1* (MIM: 605515), *LAMC3* (MIM: 604349), *MYO1E* (MIM: 601479), *PRKAR1B*, *RANBP17* (MIM: 606141), *RUFY3* (MIM: 611194), *SHANK3* (MIM: 606230), and *TRIO*.
(B) Density plots of the number of variants (intersection of FreeBayes and GATK) called in the exome-by-exome sequencing and by genome sequencing. Shown is the uniformity of calls in the genome data where only ancestry is a contributor to the difference between samples. Of note, exome data are exceedingly variable in the number of variant calls.

Table 1. Enrichment of Mutations in Putative Regulatory Elements

	Autism		**Control**				
Variant Category	**Variant Count**	**Genes Associated with Autism Risk Variants**	**Variant Count**	**Genes Associated with Autism Risk Variants**	**Fisher's One-Sided p Value**	**Confidence Interval**	**Fisher's OR**
Total	3,787	–	2,997	–	–	–	–
Noncoding Putative Regulatory							
d = 10 kb	5	*ARID1B* (2), *PRKCA*, *DSCAM*, *SCN2A*	0	–	0.05	[0.96, inf]	inf
d = 25 kb	6	*ARID1B* (2), *NR3C2*, *PRKCA*, *DSCAM*, *SCN2A*	0	–	0.03	[1.22, inf]	inf
d = 50 kb	6	*ARID1B* (2), *NR3C2*, *PRKCA*, *DSCAM*, *SCN2A*	0	–	0.03	[1.22, inf]	inf
d = 100 kb	8	*ARID1B* (2), *NR3C2*, *PRKCA*, *PHYIN*, *DSCAM*, *SCN2A*, *TRIO*	1	*DYRK1A* (MIM: 600855)	0.04	[1.05, inf]	6.34
d = 500 kb	21	*ARID1B* (2), *CACNA1D* (MIM: 114206), *CHD2* (MIM: 602119), *MYO1E* (MIM: 601479), *NR3C2*, *PRKAR1B*, *PRKCA*, *PYHIN1* (2; MIM: 612677), *SCN2A*, *SHANK3*, *WDFY3*, *DSCAM*, *PRKAR1B*, *RFX7* (MIM: 612660), *SCN2A*, *SLC6A13* (MIM: 615097), *SRCAP* (MIM: 611421), *TRIO*, *UNC45B* (MIM: 611220)	9	*DYRK1A* (3), *TMEM94*, *CACNA1D*, *CHD2*, *CHD8* (MIM: 610528), *RFX7*, *UNC45B*	0.08	[0.91, inf]	1.85
d = 1 Mb	28	*ARID1B* (2), *ASH1L* (MIM: 607999), *CACNA1D*, *CHD2*, *CREBBP* (2; MIM: 600140), *MYO1E*, *NR3C2*, *NRXN1* (MIM: 600565), *POGZ* (MIM: 614787), *PRKAR1B*, *PRKCA*, *PYHIN1* (2), *SCN2A*, *SHANK3*, *WDFY3*, *AGAP2*, *DSCAM*, *PRKAR1B*, *RFX7*, *SCN2A*, *SLC6A13*, *SRCAP*, *TRIO*, *UBE3C* (MIM: 614454), *UNC45B*	18	*CACNA1D*, *CHD2*, *CLASP1* (MIM: 605852), *DYRK1A* (3), *TMEM94* (2), *LAMC3*, *PSME4* (MIM: 607705), *SCN2A*, *TBR1* (MIM: 604616), *WDFY3*, *CHD8*, *RFX7*, *SRCAP*, *UBE3C*, *UNC45B*	0.3	[0.72, inf]	1.23

This table summarizes the counts of possible disruptive mutations (de novo SNVs or CNVs) in predicted regulatory regions between probands and unaffected (control) siblings. The analysis is limited to genes associated with autism risk according to previous evidence of de novo LGD mutations in the coding region. The nearest gene with a given distance (d) is indicated as described in the Material and Methods. Abbreviations are as follows: inf, infinity; and OR, odds ratio.

affected by simplex autism[5,32,57] (Table S15). We hypothesized that these genes associated with autism risk might harbor more noncoding putative regulatory variants in probands given that such mutations would be more likely to affect dosage, as has been observed for Mendelian diseases.[58] Because regulatory elements can exist at least as far as 1 Mb[11] away from the gene, we tested various distance intervals (d) on either side of the transcription start and end of each gene. We consistently found an excess of de novo SNV and indel variants in probands, although none reached statistical significance (lowest p = 0.27, Fisher's exact test).

We also examined CNVs for the same effect. Validation by aCGH, SNP microarray, or PCR was attempted on all de novo and private CNVs identified in the phase I genomes (n = 2,002). From this high-confidence set, we defined 1,202 validated de novo and private CNVs with at least one DNase I hypersensitive base. As with SNVs, we found a slight excess of events in probands at all distance intervals (lowest p value = 0.09 at d = 100 kb), which contained five events in probands (*DSCAM*, *FAT3* [MIM: 612483], *PRKAR1B* [MIM: 176911], *TRIO* [MIM: 601893], and *ZC3H4*) but only a single event in siblings (*PAX5* [MIM: 167414]). A combined analysis with de novo SNVs and private CNVs showed greater enrichment around genes where an excess of de novo protein-coding variants had been identified. This occurred especially in proximity to the gene (d = 25 kb [p = 0.12], d = 50 kb [p = 0.07], and d = 100 kb [p = 0.06]). In order to increase power, we tested for enrichment around autism-associated genes by using a larger set of samples sequenced locally (phase II genomes). We integrated genome sequence data from an additional 13 affected trios and 3 unaffected trios for a total of 53 autism genomes and 43 unaffected siblings or control individuals. We found modest yet statistically significant enrichment of potentially disruptive events close to genes associated with autism risk (d = 25 kb [p = 0.03], d = 50 kb [p = 0.03], and d = 100 kb [p = 0.04]; varying d shown in Table 1). Thus, three of the six tests showed nominal significance, and significance dropped off as distance increased. The set includes de novo SNVs (Table 2) and CNVs (Table 2) near *DSCAM*, *SCN2A* (MIM: 182390), *TRIO*, *NR3C2* (MIM: 600983), and *PRKCA* (MIM: 176960) and multiple events associated with *ARID1B* (MIM: 614556) (Figure 6). Replication of this effect is required and will be testable with larger sample sizes in the future.

Table 2. Variants of Interest in Autistic Individuals from 53 Families

Genomic HGVS (GRCh37)	Individual	Inheritance	Valid	Caller	Dataset	Type	Gene Exonic Splice	Putative Regulatory Variant	RefSeq HGVS
ChrX: g.154770750_154784551del	11000.p1	MP	Y	VH	phase II	CDS	*TMLHE*	N	NM_018196: c.–1–9613_181+4007del
Chr21: g.42016189_42030325del	11572.p1	MP	Y	D, GS, VH	phase I	NCS	N	*DSCAM* (d = 10 kb)*	–
Chr12: g.1948914_1984653del	11709.p1	FP	Y	GS, VH	phase II	CDS	*CACNA2D4*	N	NM_172364: c.1720–150_2551+991del
Chr6: g.157315964_157328116del	11709.p1	MP	Y	GS, VH	phase II	NCS	N	*ARID1B* (d = 10 kb)*	–
Chr2: g.166253120_166373394del	11709.p1	MP	Y	GS, VH	phase II	NCS	*CSRNP3*	*SCN2A* (d = 10 kb)*	–
Chr1: g.231828151_231933482del	11712.p1	MP	Y	GS, VH	phase II	CDS	*DISC1*	N	NM_018662: c.68–1421_1690–2372del
Chr2: g.149051133_149086337del	11712.p1	FP	Y	GS, VH	phase II	NCS	N	*MBD5* (d = 10 kb)	–
Chr2: g.233396326G>A	11729.p1	DN	Y	GATK	phase II	CDS missense	*CHRND*	N	NM_000751: c.1007G>A; NP_000742: p.Arg336Gln
Chr11: g.67926275G>A	11729.p1	DN	Y	GATK	phase II	CDS missense	*SUV420H1*	N	NM_017635: c.1538C>T; NP_060105: p.Ala513Val
Chr3: g.178916936G>A	11804.p1	DN	Y	GATK	phase II	CDS missense	*PIK3CA*	N	NM_006218: c.323G>A; NP_006209: p.Arg108His
Chr3: g.13920617_13922554del	12793.p1	MP	Y	GS,VH	phase I	CDS	*WNT7A*	N	NM_004625: c.–1241_71+626del
Chr4: g.148986808G>A	12793.p1	DN	Y	GATK	phase I	NCS	N	*NR3C2* (d = 25 kb)*	–
Chr10: g.114901076G>A	13069.p1	DN	Y	GATK, F	phase I	ESS	*TCF7L2*	N	NM_001146274: c.685+1G>A
Chr6: g.157401254C>A	13111.p1	DN	Y	GATK	phase II	NCS	N	*ARID1B* (d = 10 kb)*	–
Chr11: g.131345836_131583798del	13122.p1	FP	Y	GS, VH	phase II	NCS	*LOC101929653*	*NTM*	–
Chr16: g.6908075_7079700del	13122.p1	MP	Y	GS, VH	phase II	NCS	N	*RBFOX1* (d = 10 kb)	–
Chr5: g.14015350_14055499dup	13539.p1	MP	Y	D	phase I	NCS	N	*TRIO* (d = 100 kb)*	–
Chr5: g.122155926_122163623del	13825.p1	FP	ND	GS, VH	phase II	CDS	*SNX2*	N	NM_003100: c.1212+1208_1509+282del
Chr15: g.25088705_25117621del	13825.p1	FP	Y	GS, VH	phase II	CDS	*SNRPN*	N	NM_022805: c–13736_–578–14041del
Chr12: g.99020493T>C	13825.p1	DN	Y	GATK	phase II	CDS missense	*IKBIP*	N	NM_153687: c.349A>G; NP_710154: p.Met117Val
Chr19: g.47635921_47687660dup	13874.p1	DN	Y	D	phase I	CDS	*SAE1*	N	NM_005500: c.98+1636_734–12830dup

(*Continued on next page*)

Table 2. *Continued*

Genomic HGVS (GRCh37)	Individual	Inheritance	Valid	Caller	Dataset	Type	Gene Exonic Splice	Putative Regulatory Variant	RefSeq HGVS
Chr1: g.159038053T>C	13942.p1	DN	Y	GATK, F	phase I	NCS	N	*PYHIN1* (d = 100 kb)*	–
Chr5: g.153030052G>A	13951.p1	DN	Y	GATK, F	phase I	CDS missense	*GRIA1*	N	NM_000827: c.623G>A; NP_000818: p.Arg208His
Chr5: g.179122573_179128204del	14153.p1	DN	Y	GS, VH	phase I	CDS	*CANX*	N	–
Chr11: g.119148951G>A	14153.p1	DN	Y	GATK, F	phase I	CDS missense	*CBL*	N	NM_005188: c.1171G>A; NP_005179: p.Val391Ile
Chr5: g.175921055A>G	14153.p1	DN	Y	GATK, F	phase I	CDS missense	*FAF2*	N	NM_014613: c.539A>G; NP_055428: p.Asp180Gly
Chr7: g.79840305A>G	14370.p1	DN	Y	GATK, F	phase I	CDS missense	*GNAI1*	N	NM_002069: c.611A>G; NP_002060: p.Gln204Arg
Chr17: g.64410805C>T	14637.p1	DN	Y	GATK, F	phase I	NCS	N	*PRKCA* (d = 10 kb)*	–

"Genomic HGVS" lists the genomic HGVS information for the variant. "Individual" is the individual ID of the person with the event. "Inheritance" indicates the inheritance (MP, mother to proband; FP, father to proband; or DN, de novo). "Valid" indicates whether the event was validated by orthogonal methods (Y, yes; ND, not determined; or ˆ, published previously). "Caller" is the variant-calling program that detected this event (D, dCGH; F, FreeBayes; GS, GenomeSTRiP; and/or VH, VariationHunter). "Dataset" indicates whether the individual was part of phase I or phase II genome families in this study. "Type" indicates the variant type (NCS, noncoding sequence [putative regulatory]; CDS, coding sequence; CDS missense, coding missense; or ESS, essential splice site). "Gene exonic splice" indicates the gene with the exonic or splice-site mutation (N, no). In the "putative regulatory variant" column, d refers to the minimal distance as defined in the Material and Methods, and an asterisk indicates that the variant is in a gene where an enrichment of de novo mutations has been identified in autism. "RefSeq HGVS" values were calculated with Alamut v.2.7.1. and are indicated for mRNA and protein where available.

Finally, we focused on integrating all potential disease-related CNV, SNV, and indel events in our set of 53 autism-affected families. In addition to identifying de novo and private mutations in putative regulatory elements of genes associated with autism risk, we identified and validated gene-disruptive CNVs in neurodevelopmental genes (*DISC1* [MIM: 605210], *WNT7A* [MIM: 601570], *RBFOX1* [MIM: 605104], and *MBD5* [MIM: 611472]). We also validated smaller de novo CNVs and SNV exon-specific mutations missed by exome sequencing in likely candidate genes (e.g., *CANX*, *SAE1*, and *PIK3CA* [MIM: 171834]) according to the literature. The evidence and significance of each are discussed in detail below. Given that autism involves a well-appreciated sex bias favoring males, we considered the yield among four different proband-sibling gender combinations (male-male, male-female, female-male, and female-female) where applicable. In this analysis (Table S16), families were scored as having a candidate event in a gene associated with autism mutational burden, a candidate event in another gene, other events, or no events. Excluding two control families in whom potential pathogenic exonic events had been previously identified, we identified 16 families (31.3%) containing largely private or de novo events within genes previously associated with autism or neurodevelopmental disease; nine families (17.6%) in particular carried potentially high-impact variants (Figure 6). Among the latter, at least five probands (9.8%) were deemed to carry multiple high-impact variants, often as a result of transmission from both parents or of multiple de novo events.

In Vivo Functional Testing of *DSCAM* Deletion Interval

Although DNase I hypersensitivity sites are enriched with noncoding regulatory DNA, their functional potential can only be determined through experimentation. We selected one of the smallest CNVs (14 kb *DSCAM* deletion interval from family 11572), which contained 12 CNS DNase I hypersensitivity sites, and assayed its potential to direct tissue-dependent reporter expression in a previously described transgenic zebrafish assay[51,52] (see Material and Methods). We synthesized nine sequence intervals (150–630 bp), corresponding to either one or two of the 12 CNS DNase I hypersensitive sites within the interval (Figure 7; see Material and Methods). Our analysis indicated that all nine constructs directed reporter expression in the CNS of 48 hpf G0 mosaic zebrafish embryos (Table 3). Although the lower threshold for reporting CNS positive expression only required signal to be detected in ≥20% of injected embryos, all constructs comfortably exceeded this threshold (range 49%–73%). Expression was seen consistently across a variety of CNS structures, including the forebrain, midbrain, hindbrain, spinal cord, olfactory placodes, and amacrine cells (Figure 7). We note that expression outside of the CNS was not consistently detected for any of the constructs, providing further evidence of the specificity. These findings are consistent

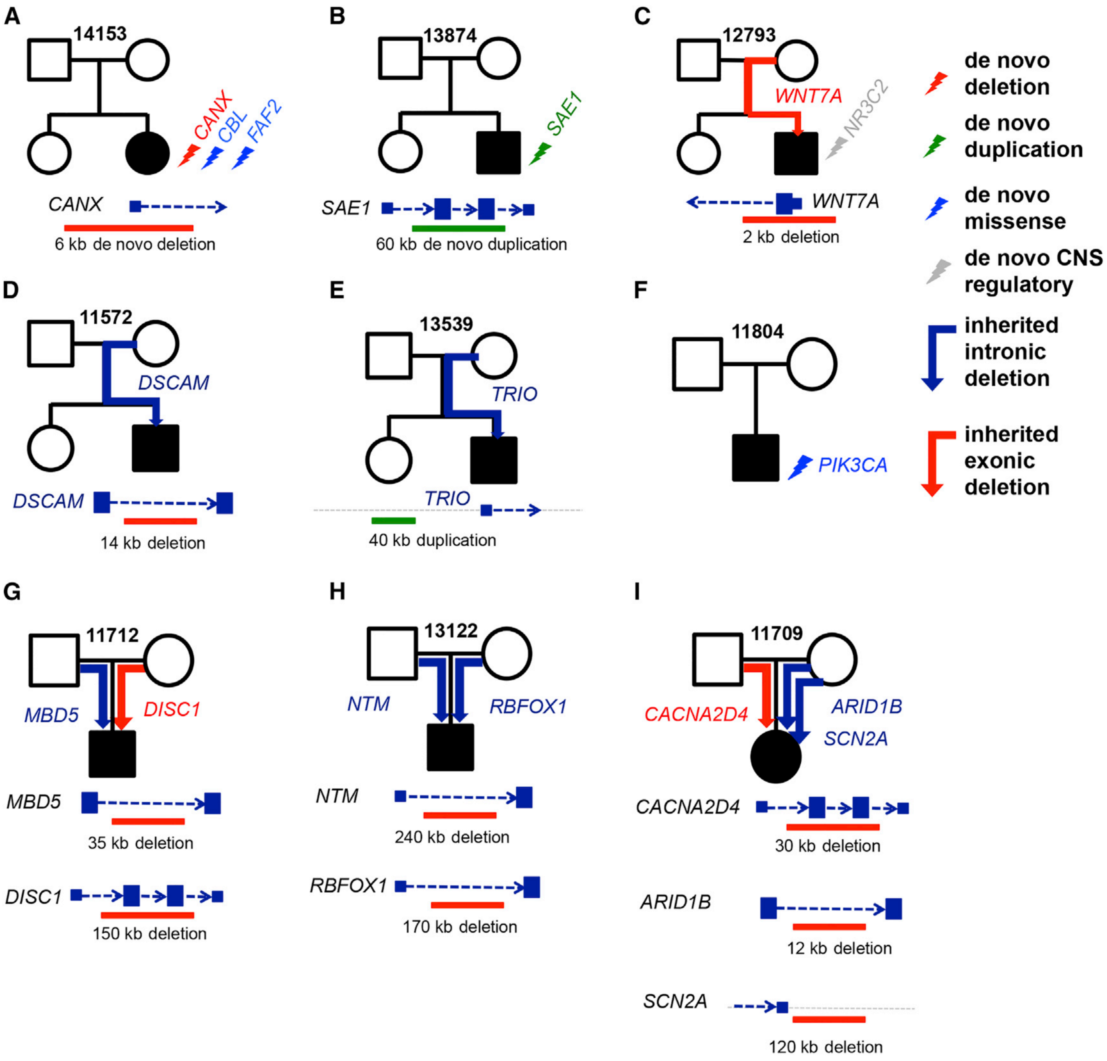

Figure 6. All Variants Shown for Each Family Were Validated by Appropriate Methods

(A) Family 14153. The events are a de novo exonic deletion of the promoter and first exon of *CANX* and two de novo missense SNVs in *CBL* (MIM: 165360) and *FAF2*. The location of the de novo deletion is also shown with respect to *CANX*.

(B) Family 13874. The event is a de novo exonic duplication in *SAE1*. Furthermore, we provided a mock representation of the de novo duplication with respect to *SAE1*.

(C) Family 12793. The event is a promoter and exonic *WNT7A* deletion passed from the mother to the male proband. As shown in the mock representation of the inherited deletion, it removes the 5′ UTR and the first exon of *WNT7A*. This proband and the mother both have macrocephaly, which is in concordance with maternally inherited deletion of *WNT7A*.

(D) Family 11572. The event is a *DSCAM* deletion encompassing CNS DNase I hypersensitive sites passed from the mother to the male proband. This individual also suffers from nonfebrile seizures, in concordance with disruption of *DSCAM*.

(E) Family 13539. The event is a duplication upstream of *TRIO*. It encompasses CNS DNase I hypersensitive sites and was passed from the mother to the male proband.

(F) Family 11804. A conserved missense de novo mutation (phyloP = 2.57) was found in *PIK3CA*. This individual has macrocephaly, which is in concordance with disruption of *PIK3CA*.

(G) Family 11712. We found a maternally inherited rare, private exonic deletion of parts of *DISC1* and a 35 kb paternally inherited rare intronic deletion of *MBD5*. The deletion affecting *DISC1* is around 150 kb, deletes a few coding exons of this gene, and is not seen in over 15,000 genotyped control individuals.

(H) Family 13122. We found two large rare deletions that intersect *NTM* and *RBFOX1*—one inherited from the father and the other inherited from the mother. The maternally inherited rare deletion is 240 kb and deletes most of the first intron of *NTM*. This is an extremely rare deletion, given that it was not observed in over 15,000 control individuals. The paternally inherited rare deletion is 170 kb and deletes an intron of *RBFOX1*.

(I) Family 11709. We found three rare, private deletions affecting genes of interest. First, we found a 30 kb paternally inherited rare, private exonic deletion of *CACNA2D4*. We also found two maternally inherited rare, private deletions that affect genes of interest. One is a 120 kb exonic rare and private deletion less than 5 kb downstream of *SCN2A*, and the other is a 12 kb rare deletion of an intron of *ARID1B*.

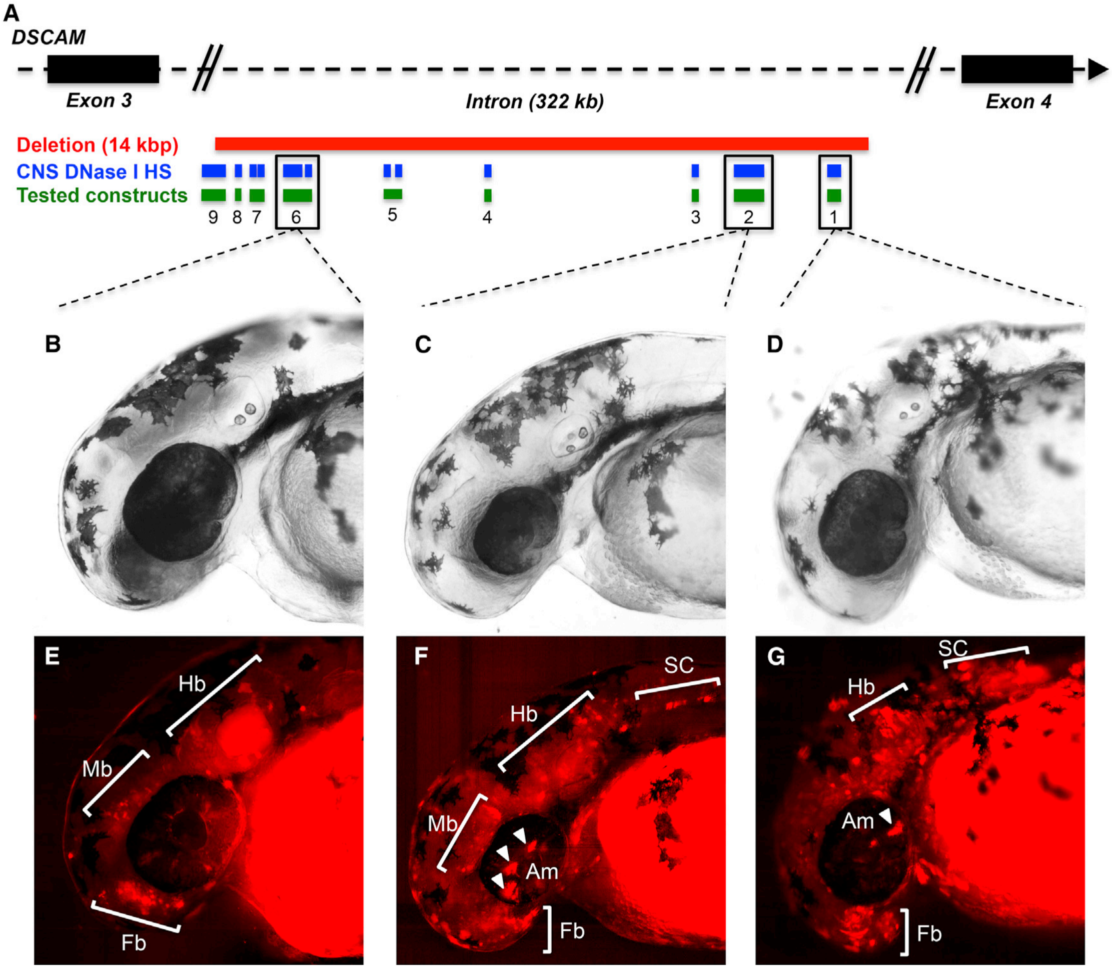

Figure 7. Functional Analysis of CNS DNase I Hypersensitivity Sites in the *DSCAM* Deletion
(A) Schematic of the 14 kb *DSCAM* deletion observed in family 11572. The diagram illustrates the 12 DNase I hypersensitivity sites (HSs) contained within the deletion, as well as the nine sequence intervals encompassing them. These sequence intervals were tested for their potential to direct reporter expression.
(B–D) Bright-field images of representative 48 hpf mosaic zebrafish embryos injected with DSCAM-6 (B), DSCAM-2 (C), and DSCAM-1 (D).
(E–G) tdTomato expression in representative 48 hpf mosaic embryos injected with DSCAM-6 (E), DSCAM-2 (F), and DSCAM-1 (G). Expression was seen in the forebrain (E–G), hindbrain (E–G), midbrain (E and F), spinal cord (F and G), and amacrine cells (F and G).

with our hypothesis that the sequences within the 14 kb *DSCAM* deletion have regulatory potential that affects CNS biology. Analyses of reporter expression in stable transgenic lines will be needed for further validating this initial finding and refining our understanding of the neuronal populations in which these sequences can function.

Discussion

In this study, we fully sequenced the genomes of 53 families who are affected by simplex autism and in whom de novo LGD mutations and large CNVs had not been detected by previous exome sequencing and microarray analysis. By this approach, we hypothesized that we would identify disease-associated events mapping to noncoding regions likely to affect gene regulation. We focused on de novo and rare inherited SNVs, indels, and CNVs identified with multiple callers in an effort to establish a set of best practices. It is critical to use a number of high-quality callers to detect variation given that no caller, at this time, is able to detect all relevant variants. In the case of SNVs, we applied both FreeBayes and GATK. The benefits of using multiple callers are twofold. First, when a variant is found by both callers, the VR is very high (89.1%), providing a very high-confidence set. Second, each caller is able to detect variants that the other missed. In our study of 40 quads, an additional 2,567 and 91 de novo and 133,058 and 57,974 private variant calls were detected by GATK alone and FreeBayes alone, respectively. These additional calls will be critical for discovering disease-related variants in affected individuals, although additional validation is required. For CNVs, especially, it is necessary to apply methods based on both read depth and read pairs. Similarly, implementing multiple de novo SNV callers

Table 3. Number of Positive Mosaic Embryos per Zebrafish Assay

Construct	Positive Mosaic Embryos	Structures with Expression
DSCAM-1	151/207 (73%)	Fb, Hb, Am, SC
DSCAM-2	129/211 (61%)	Fb, Mb, Hb, SC
DSCAM-3	127/214 (59%)	Fb, Mb, Hb
DSCAM-4	97/161 (60%)	Fb, Hb, Am, OP
DSCAM-5	118/180 (66%)	Fb, Hb, Am
DSCAM-6	80/162 (49%)	Fb, Mb, Hb, Am, SC
DSCAM-7	128/182 (72%)	Fb, Hb
DSCAM-8	125/174 (72%)	Fb
DSCAM-9	118/189 (62%)	Hb, SC

Specific brain structures with expression are indicated. Abbreviations are as follows: Fb, forebrain; Mb, midbrain; Hb, hindbrain; Am, amacrine cells; SC, spinal cord; and OP, plfactory placode.

significantly increases sensitivity. In this study, we combined the well-established practice of using a machine-learning-based approach to discover a high-quality dataset with the benefit of additional variants by a genotype likelihood-based approach.

In our study, we had access to WES and WGS data generated with the same sequencing platform for 149 of the individuals. This comparison differs from that of a previously published study of genome sequencing in intellectual disability,[12] where the comparison was made with very different platforms (e.g., Complete Genomics WGS and SOLiD WES). On the basis of our comparisons of WGS and WES, we hypothesize that the heterogeneity in sequencing platforms most likely led to an overestimate of the utility of genome sequencing data, in part because the SOLiD data had much poorer representation of the exome (~50% fewer variants than would be expected on the basis of more recent experiments).[8,13] In addition, the comparison presented here is more direct because we controlled for differences in discovery methods by calling SNVs and indels calls with the exact same software packages. Our study has found a benefit of using both WES and WGS for discovering SNVs and indels, as in a previously reported study,[13] and highlights to a much greater extent the utility of CNV discovery within genome data and its superiority over exome sequencing in detecting variants. Although exome sequencing is very cost efficient, we found that genome sequencing increased sensitivity within protein-coding regions in that it recovered on average two million more bases than WES. In particular, this addition was in regions of higher GC content and allowed access to additional sequence in 1,854 genes previously missed in most samples by exome sequencing. SNV and indel calling was much more uniform in an analysis of genome sequencing data—the only noticeable shift in variation numbers was due to ancestry. Remarkably, the greatest benefit came from the discovery of small CNVs corresponding to single-exon events that cannot be reliably detected through exome sequence data.[7] Importantly, these differences are in addition to the potential importance to be derived from the vastly increased sensitivity WGS provides over WES in analysis of noncoding transcribed and intergenic sequences. Nevertheless, combining both WES and WGS datasets achieves maximal sensitivity in discovering variants in coding DNA sequence (CDS). Our data suggest that integrating WES has the potential to increase SNV yield within protein-coding regions by 5%–10%, partly because of the higher sequence coverage afforded by WES. In lieu of combining WES and WGS, an alternate approach would be to perform deeper WGS sequencing,[12] especially as the cost of WGS declines and WES is ultimately abandoned.

Among the de novo mutations in the 53 families, we discovered a 6 kb deletion of the first exon and promoter of calnexin (*CANX*) in proband 14153.p1. *CANX* binds calcium and associates with N-linked glycoproteins in the endoplasmic reticulum, where it is thought to function as a molecular chaperone. The gene is highly expressed in human neurons derived from induced pluripotent stem cells[59] and has been predicted to be a protein-protein interaction hub associated with de novo mutations in individuals with schizophrenia.[60] Interestingly, this particular affected female individual has the highest burden of de novo mutations (n = 3) in this study and might be an example of the female protective effect, whereby the development of autism requires a higher genetic burden.[61,62] In another family (13874), we discovered a larger de novo duplication (52 kb) affecting multiple exons of SUMO-activating enzyme unit 1, *SAE1*. *SAE1* encodes one of the key proteins associated with the sumoylation pathway,[63] which plays a role, among many others, in neuronal differentiation and synapse formation.[64] Remarkably, four additional individuals carrying duplications of this locus have been reported previously in autism,[65,66] suggesting that a recurrent duplication might be associated with autism risk (Figure S16). We also discovered de novo missense mutations in genes associated with the glutamate receptor excitatory pathway in proband 13951.p1 (*GRIA1* [MIM: 138248]) and proband 14370.p1 (*GNAI1* [MIM: 139310]), as well as de novo mutations in two genes (*CHRND* [MIM: 100720] and *SUV420H1* [MIM: 610881]) in proband 11729.p1 and a severe missense mutation (c.323G>A [p.Arg108His]) in the first exon of *PIK3CA*, missed by exome sequencing, in proband 11804.p1. Missense mutations of this gene have been previously associated with megalencephaly-capillary malformation-polymicrogyria (MCAP syndrome [MIM: 602501]),[67] megalencephaly, hemimegalencephaly, and focal cortical dysplasia.[68,69] The autistic proband in this case was macrocephalic with a head circumference of 62 cm (5.6 SDs above the mean[70]) and a height of 147 cm (age 10 years).

Among potential inherited risk variants, we discovered that a private deletion of the promoter and first exon of *WNT7A* was transmitted maternally to a male proband (12793.p1). This CNV was only detected by read-pair analysis and was probably missed by WES because of its size (2 kb) and very high GC content (~79%). WGS read-depth analysis, SNP microarray, and aCGH validation failed to detect or validate this event. PCR and sequencing of the breakpoints were the only experimental methods that confirmed the deletion. *WNT7A* is a critical gene in both cell proliferation and Wnt signaling; it has been implicated in diverse neuronal processes, including neural stem cell renewal, synapse formation, axon guidance, and neuronal progenitor cell progression.[71] Whereas only the proband has a diagnosis of autism, both the proband and his mother have macrocephaly, and the proband has complications of gastrointestinal dysfunction—phenotypes seen in other genes associated with Wnt signaling.[72] We also identified that a small deletion (14 kb) within noncoding putative regulatory DNA of *DSCAM* was transmitted from the mother to the male proband in family 11572. *DSCAM* is one of two genes associated with neurocognitive dysfunction with Down syndrome (MIM: 190685), and multiple de novo and inherited CNVs disrupting this gene have been reported among cases of autism.[7,45] For this particular deletion, 19% of the locus is characterized as DNase I hypersensitive, representing open chromatin; we hypothesize that the deletion is likely to have an effect on gene regulation. The proband in this family has a history of seizures—a phenotype also found in mice homozygous for loss-of-function mutations in this gene.[73] In addition, our modeling in zebrafish showed that nine of nine tested CNS DNase I hypersensitive sites drive expression in vivo in the CNS (Figure 7 and Figure S17). We also found that a 40 kb noncoding putative regulatory duplication upstream of the gene *TRIO* was transmitted from the mother to the male proband in family 13539. *TRIO* encodes a rho-guanine nucleotide exchange factor and has been observed to be disrupted by new mutations in children with autism and intellectual disability.[57,74] Although this deletion does not affect exons, we note that 8% of the locus is DNase I hypersensitive and carries a robust H3K27AC signal, demarcating active regulatory elements.[10] Although validating the effect of these smaller CNVs will require additional functional work, the association between such private or de novo damaging events and genes already implicated in autism makes them particularly appealing candidates. Most of the smaller CNVs associated with autism risk in this study were transmitted from the mother to the male proband, consistent with the maternal transmission bias observed for large CNVs and now inherited private gene-disruptive SNVs in autism.[7,61,75]

In five (~10%) families, we identified probands carrying multiple high-risk mutations, potentially consistent with a more complex oligogenic model of autism risk.[76] Autism proband 11712.p1, for example, carries a maternally inherited 120 kb genic deletion of *DISC1*, a gene strongly associated with schizophrenia (MIM: 181500) and bipolar disorder (MIM: 125480)[77,78]—as well as a 35 kb paternally inherited private intronic deletion of *MBD5* (MIM: 611472), a gene previously implicated in neurodevelopmental disorders.[79,80] In male proband 13122.p1, we identified two large private CNVs within the introns of neurodevelopmental genes *NTM* (MIM: 607938)[81]) and *RBFOX1*[82–84] (Figure 6). One female autistic proband, 13825.p1, carries a de novo missense mutation in *IKBIP* (MIM: 609861), in addition to a maternally inherited deletion of *SNX2* (MIM: 605929) and paternally inherited 29 kb deletion involving a portion of the 5′ UTR of *SNRPN* (MIM: 182279), a maternal imprinted gene associated with Prader-Willi syndrome.[85] In another female proband, 11709.p1, we found three rare, private deletions affecting neurodevelopmental genes. These include two maternally inherited deletions, a 12 kb intronic deletion of *ARID1B*, and a 120 kb deletion mapping within 5 kb of *SCN2A*, as well as a 30 kb paternally inherited rare exonic deletion of *CACNA2D4* (MIM: 608171). The latter CNV is significantly more abundant in individuals with pediatric developmental delay and autism spectrum disorders than in control individuals ($OR = 2.75$, $p = 0.03$).[43] These findings suggest that smaller CNVs affecting single exons and regulatory elements in genes associated with dosage imbalance and autism risk will be an important area of focus for future investigation.

Accession Numbers

The accession number for the phase I genome sequences reported in this paper is SFARI Base: SFARI_SSC_WGS_P. The accession numbers for the phase II genome sequences are SFARI Base: SFARI_SSC_WGS_trioP and dbGaP: phs001035. The variant calls reported in this paper are available in the National Database for Autism Research under accession number NDAR: 10.15154/1226523.

Supplemental Data

Supplemental Data include 17 figures and 16 tables and can be found with this article online at http://dx.doi.org/10.1016/j.ajhg.2015.11.023.

Conflicts of Interest

E.E.E. is on the scientific advisory board of DNAnexus Inc. and is a consultant for Kunming University of Science and Technology as part of the 1000 China Talent Program.

Acknowledgments

We thank T. Brown for assistance in editing this manuscript. This work was supported by grants from the Simons Foundation (SFARI 336475 to E.E.E.), National Institute of Child Health and Development (HHSN267200700021C to J.M.S.), (HHSN275200800015C and HHSN267200700023C to E.M.F.), National Institute of Neurological Disorders and Stroke (NS062972 to A.S.M.), National Institute of General Medical Sciences (predoctoral training grant 5T32GM07814 to P.W.H.), and National Human Genome Research Institute (postdoctoral training grant 2T32HG000035 to T.N.T.). We also thank Dr. Daniela Witten for advice on statistical testing of regulatory elements and Dr. Bradley Coe for information on CNVs from his previous publication. We thank Natalia Volfovsky, Alex Lash, and Malcolm Mallardi from the Simons Foundation for help with depositing genome data to SFARI Base and Colleen Davis for help with depositing genome data to dbGaP. We are grateful to all of the families at the participating Simons Simplex Collection (SSC) sites, as well as the principal investigators (A. Beaudet, R. Bernier, J. Constantino, E. Cook, E. Fombonne, D. Geschwind, R. Goin-Kochel, E. Hanson, D. Grice, A. Klin, D. Ledbetter, C. Lord, C. Martin, D. Martin, R. Maxim, J. Miles, O. Ousley, K. Pelphrey, B. Peterson, J. Piggot, C. Saulnier, M. State, W. Stone, J. Sutcliffe, C. Walsh, Z. Warren, and E. Wijsman). We appreciate receiving access to phenotypic data on Simons Foundation Autism Research Initiative (SFARI) Base. Approved researchers can obtain the SSC population dataset described in this study by applying at SFARI Base (see Web Resources). E.E.E. is an investigator of the Howard Hughes Medical Institute.

Received: August 5, 2015
Accepted: November 25, 2015
Published: December 31, 2015

Web Resources

The URLs for data presented herein are as follows:

1000 Genomes GRCh37 assembly, ftp://ftp.1000genomes.ebi.ac.uk/vol1/ftp/technical/reference/human_g1k_v37.fasta.gz
dbGaP, http://www.ncbi.nlm.nih.gov/gap
National Database for Autism Research (NDAR) study, http://dx.doi.org/10.15154/1226523
OMIM, http://www.omim.org
RefSeq, http://www.ncbi.nlm.nih.gov/refseq/
SFARI Base, https://base.sfari.org/
SFARI Base WGS data, https://sfari.org/resources/autism-cohorts/simons-simplex-collection

References

1. Steffenburg, S., Gillberg, C., Hellgren, L., Andersson, L., Gillberg, I.C., Jakobsson, G., and Bohman, M. (1989). A twin study of autism in Denmark, Finland, Iceland, Norway and Sweden. J. Child Psychol. Psychiatry *30*, 405–416.
2. Bailey, A., Le Couteur, A., Gottesman, I., Bolton, P., Simonoff, E., Yuzda, E., and Rutter, M. (1995). Autism as a strongly genetic disorder: evidence from a British twin study. Psychol. Med. *25*, 63–77.
3. Verkerk, A.J., Pieretti, M., Sutcliffe, J.S., Fu, Y.H., Kuhl, D.P., Pizzuti, A., Reiner, O., Richards, S., Victoria, M.F., Zhang, F.P., et al. (1991). Identification of a gene (FMR-1) containing a CGG repeat coincident with a breakpoint cluster region exhibiting length variation in fragile X syndrome. Cell *65*, 905–914.
4. Amir, R.E., Van den Veyver, I.B., Wan, M., Tran, C.Q., Francke, U., and Zoghbi, H.Y. (1999). Rett syndrome is caused by mutations in X-linked MECP2, encoding methyl-CpG-binding protein 2. Nat. Genet. *23*, 185–188.
5. Iossifov, I., O'Roak, B.J., Sanders, S.J., Ronemus, M., Krumm, N., Levy, D., Stessman, H.A., Witherspoon, K.T., Vives, L., Patterson, K.E., et al. (2014). The contribution of de novo coding mutations to autism spectrum disorder. Nature *515*, 216–221.
6. Petrovski, S., Wang, Q., Heinzen, E.L., Allen, A.S., and Goldstein, D.B. (2013). Genic intolerance to functional variation and the interpretation of personal genomes. PLoS Genet. *9*, e1003709.
7. Krumm, N., Turner, T.N., Baker, C., Vives, L., Mohajeri, K., Witherspoon, K., Raja, A., Coe, B.P., Stessman, H.A., He, Z.X., et al. (2015). Excess of rare, inherited truncating mutations in autism. Nat. Genet. *47*, 582–588.
8. Yuen, R.K., Thiruvahindrapuram, B., Merico, D., Walker, S., Tammimies, K., Hoang, N., Chrysler, C., Nalpathamkalam, T., Pellecchia, G., Liu, Y., et al. (2015). Whole-genome sequencing of quartet families with autism spectrum disorder. Nat. Med. *21*, 185–191.
9. Thomas, D.J., Rosenbloom, K.R., Clawson, H., Hinrichs, A.S., Trumbower, H., Raney, B.J., Karolchik, D., Barber, G.P., Harte, R.A., Hillman-Jackson, J., et al.; ENCODE Project Consortium (2007). The ENCODE Project at UC Santa Cruz. Nucleic Acids Res. *35*, D663–D667.
10. ENCODE Project Consortium (2004). The ENCODE (ENCyclopedia Of DNA Elements) Project. Science *306*, 636–640.
11. Lettice, L.A., Heaney, S.J., Purdie, L.A., Li, L., de Beer, P., Oostra, B.A., Goode, D., Elgar, G., Hill, R.E., and de Graaff, E. (2003). A long-range Shh enhancer regulates expression in the developing limb and fin and is associated with preaxial polydactyly. Hum. Mol. Genet. *12*, 1725–1735.
12. Gilissen, C., Hehir-Kwa, J.Y., Thung, D.T., van de Vorst, M., van Bon, B.W., Willemsen, M.H., Kwint, M., Janssen, I.M., Hoischen, A., Schenck, A., et al. (2014). Genome sequencing identifies major causes of severe intellectual disability. Nature *511*, 344–347.
13. Belkadi, A., Bolze, A., Itan, Y., Cobat, A., Vincent, Q.B., Antipenko, A., Shang, L., Boisson, B., Casanova, J.-L., and Abel, L. (2015). Whole-genome sequencing is more powerful than whole-exome sequencing for detecting exome variants. Proc. Natl. Acad. Sci. USA *112*, 5473–5478.
14. Lelieveld, S.H., Spielmann, M., Mundlos, S., Veltman, J.A., and Gilissen, C. (2015). Comparison of Exome and Genome Sequencing Technologies for the Complete Capture of Protein-Coding Regions. Hum. Mutat. *36*, 815–822.
15. Iossifov, I., Ronemus, M., Levy, D., Wang, Z., Hakker, I., Rosenbaum, J., Yamrom, B., Lee, Y.H., Narzisi, G., Leotta, A., et al. (2012). De novo gene disruptions in children on the autistic spectrum. Neuron *74*, 285–299.
16. Sanders, S.J., Murtha, M.T., Gupta, A.R., Murdoch, J.D., Raubeson, M.J., Willsey, A.J., Ercan-Sencicek, A.G., DiLullo, N.M., Parikshak, N.N., Stein, J.L., et al. (2012). De novo mutations revealed by whole-exome sequencing are strongly associated with autism. Nature *485*, 237–241.
17. O'Roak, B.J., Deriziotis, P., Lee, C., Vives, L., Schwartz, J.J., Girirajan, S., Karakoc, E., Mackenzie, A.P., Ng, S.B., Baker, C., et al. (2011). Exome sequencing in sporadic autism spectrum disorders identifies severe de novo mutations. Nat. Genet. *43*, 585–589.
18. O'Roak, B.J., Vives, L., Girirajan, S., Karakoc, E., Krumm, N., Coe, B.P., Levy, R., Ko, A., Lee, C., Smith, J.D., et al. (2012). Sporadic autism exomes reveal a highly interconnected protein network of de novo mutations. Nature *485*, 246–250.
19. Sanders, S.J., Ercan-Sencicek, A.G., Hus, V., Luo, R., Murtha, M.T., Moreno-De-Luca, D., Chu, S.H., Moreau, M.P., Gupta, A.R., Thomson, S.A., et al. (2011). Multiple recurrent de novo CNVs, including duplications of the 7q11.23 Williams syndrome region, are strongly associated with autism. Neuron *70*, 863–885.

20. Levy, D., Ronemus, M., Yamrom, B., Lee, Y.H., Leotta, A., Kendall, J., Marks, S., Lakshmi, B., Pai, D., Ye, K., et al. (2011). Rare de novo and transmitted copy-number variation in autistic spectrum disorders. Neuron *70*, 886–897.
21. Hach, F., Hormozdiari, F., Alkan, C., Hormozdiari, F., Birol, I., Eichler, E.E., and Sahinalp, S.C. (2010). mrsFAST: a cache-oblivious algorithm for short-read mapping. Nat. Methods *7*, 576–577.
22. Manichaikul, A., Mychaleckyj, J.C., Rich, S.S., Daly, K., Sale, M., and Chen, W.M. (2010). Robust relationship inference in genome-wide association studies. Bioinformatics *26*, 2867–2873.
23. Girirajan, S., Brkanac, Z., Coe, B.P., Baker, C., Vives, L., Vu, T.H., Shafer, N., Bernier, R., Ferrero, G.B., Silengo, M., et al. (2011). Relative burden of large CNVs on a range of neurodevelopmental phenotypes. PLoS Genet. *7*, e1002334.
24. Celestino-Soper, P.B., Shaw, C.A., Sanders, S.J., Li, J., Murtha, M.T., Ercan-Sencicek, A.G., Davis, L., Thomson, S., Gambin, T., Chinault, A.C., et al. (2011). Use of array CGH to detect exonic copy number variants throughout the genome in autism families detects a novel deletion in TMLHE. Hum. Mol. Genet. *20*, 4360–4370.
25. McKenna, A., Hanna, M., Banks, E., Sivachenko, A., Cibulskis, K., Kernytsky, A., Garimella, K., Altshuler, D., Gabriel, S., Daly, M., and DePristo, M.A. (2010). The Genome Analysis Toolkit: a MapReduce framework for analyzing next-generation DNA sequencing data. Genome Res. *20*, 1297–1303.
26. Van der Auwera, G.A., Carneiro, M.O., Hartl, C., Poplin, R., Del Angel, G., Levy-Moonshine, A., Jordan, T., Shakir, K., Roazen, D., Thibault, J., et al. (2013). From FastQ data to high confidence variant calls: the Genome Analysis Toolkit best practices pipeline. Curr. Protoc. Bioinformatics *11*, 11.10.11–11.10.33.
27. Garrison, E.M.G. (2012). Haplotype-based variant detection from short-read sequencing. arXiv, arXiv:1207.3907, http://arxiv.org/abs/1207.3907.
28. Rimmer, A., Phan, H., Mathieson, I., Iqbal, Z., Twigg, S.R., Wilkie, A.O., McVean, G., and Lunter, G.; WGS500 Consortium (2014). Integrating mapping-, assembly- and haplotype-based approaches for calling variants in clinical sequencing applications. Nat. Genet. *46*, 912–918.
29. Liu, Y., Li, B., Tan, R., Zhu, X., and Wang, Y. (2014). A gradient-boosting approach for filtering de novo mutations in parent-offspring trios. Bioinformatics *30*, 1830–1836.
30. Wei, Q., Zhan, X., Zhong, X., Liu, Y., Han, Y., Chen, W., and Li, B. (2015). A Bayesian framework for de novo mutation calling in parents-offspring trios. Bioinformatics *31*, 1375–1381.
31. Li, H., and Durbin, R. (2010). Fast and accurate long-read alignment with Burrows-Wheeler transform. Bioinformatics *26*, 589–595.
32. O'Roak, B.J., Vives, L., Fu, W., Egertson, J.D., Stanaway, I.B., Phelps, I.G., Carvill, G., Kumar, A., Lee, C., Ankenman, K., et al. (2012). Multiplex targeted sequencing identifies recurrently mutated genes in autism spectrum disorders. Science *338*, 1619–1622.
33. Robinson, J.T., Thorvaldsdóttir, H., Winckler, W., Guttman, M., Lander, E.S., Getz, G., and Mesirov, J.P. (2011). Integrative genomics viewer. Nat. Biotechnol. *29*, 24–26.
34. Michaelson, J.J., Shi, Y., Gujral, M., Zheng, H., Malhotra, D., Jin, X., Jian, M., Liu, G., Greer, D., Bhandari, A., et al. (2012). Whole-genome sequencing in autism identifies hot spots for de novo germline mutation. Cell *151*, 1431–1442.
35. Ng, S.B., Turner, E.H., Robertson, P.D., Flygare, S.D., Bigham, A.W., Lee, C., Shaffer, T., Wong, M., Bhattacharjee, A., Eichler, E.E., et al. (2009). Targeted capture and massively parallel sequencing of 12 human exomes. Nature *461*, 272–276.
36. Sudmant, P.H., Kitzman, J.O., Antonacci, F., Alkan, C., Malig, M., Tsalenko, A., Sampas, N., Bruhn, L., Shendure, J., and Eichler, E.E.; 1000 Genomes Project (2010). Diversity of human copy number variation and multicopy genes. Science *330*, 641–646.
37. Handsaker, R.E., Korn, J.M., Nemesh, J., and McCarroll, S.A. (2011). Discovery and genotyping of genome structural polymorphism by sequencing on a population scale. Nat. Genet. *43*, 269–276.
38. Hormozdiari, F., Hajirasouliha, I., McPherson, A., Eichler, E.E., and Sahinalp, S.C. (2011). Simultaneous structural variation discovery among multiple paired-end sequenced genomes. Genome Res. *21*, 2203–2212.
39. Fromer, M., Moran, J.L., Chambert, K., Banks, E., Bergen, S.E., Ruderfer, D.M., Handsaker, R.E., McCarroll, S.A., O'Donovan, M.C., Owen, M.J., et al. (2012). Discovery and statistical genotyping of copy-number variation from whole-exome sequencing depth. Am. J. Hum. Genet. *91*, 597–607.
40. Krumm, N., Sudmant, P.H., Ko, A., O'Roak, B.J., Malig, M., Coe, B.P., Quinlan, A.R., Nickerson, D.A., and Eichler, E.E.; NHLBI Exome Sequencing Project (2012). Copy number variation detection and genotyping from exome sequence data. Genome Res. *22*, 1525–1532.
41. Münz, M., Ruark, E., Renwick, A., Ramsay, E., Clarke, M., Mahamdallie, S., Cloke, V., Seal, S., Strydom, A., Lunter, G., and Rahman, N. (2015). CSN and CAVA: variant annotation tools for rapid, robust next-generation sequencing analysis in the clinical setting. Genome Med. *7*, 76.
42. Sherry, S.T., Ward, M., and Sirotkin, K. (1999). dbSNP-database for single nucleotide polymorphisms and other classes of minor genetic variation. Genome Res. *9*, 677–679.
43. Coe, B.P., Witherspoon, K., Rosenfeld, J.A., van Bon, B.W., Vulto-van Silfhout, A.T., Bosco, P., Friend, K.L., Baker, C., Buono, S., Vissers, L.E., et al. (2014). Refining analyses of copy number variation identifies specific genes associated with developmental delay. Nat. Genet. *46*, 1063–1071.
44. John, S., Sabo, P.J., Thurman, R.E., Sung, M.H., Biddie, S.C., Johnson, T.A., Hager, G.L., and Stamatoyannopoulos, J.A. (2011). Chromatin accessibility pre-determines glucocorticoid receptor binding patterns. Nat. Genet. *43*, 264–268.
45. O'Roak, B.J., Stessman, H.A., Boyle, E.A., Witherspoon, K.T., Martin, B., Lee, C., Vives, L., Baker, C., Hiatt, J.B., Nickerson, D.A., et al. (2014). Recurrent de novo mutations implicate novel genes underlying simplex autism risk. Nat. Commun. *5*, 5595.
46. Liaw, A., and Wiener, M. (2002). Classification and Regression by randomForest. R News *2*, 18–22.
47. Hothorn, T., Hornik, K., and Zeileis, A. (2006). Unbiased Recursive Partitioning: A Conditional Inference Framework. J. Comput. Graph. Stat. *15*, 651–674.
48. Ritchie, M.E., Carvalho, B.S., Hetrick, K.N., Tavaré, S., and Irizarry, R.A. (2009). R/Bioconductor software for Illumina's Infinium whole-genome genotyping BeadChips. Bioinformatics *25*, 2621–2623.
49. Scharpf, R.B., Irizarry, R.A., Ritchie, M.E., Carvalho, B., and Ruczinski, I. (2011). Using the R Package crlmm for Genotyping and Copy Number Estimation. J. Stat. Softw. *40*, 1–32.
50. Fu, C., Wehr, D.R., Edwards, J., and Hauge, B. (2008). Rapid one-step recombinational cloning. Nucleic Acids Res. *36*, e54.

51. Fisher, S., Grice, E.A., Vinton, R.M., Bessling, S.L., and McCallion, A.S. (2006). Conservation of RET regulatory function from human to zebrafish without sequence similarity. Science *312*, 276–279.
52. Fisher, S., Grice, E.A., Vinton, R.M., Bessling, S.L., Urasaki, A., Kawakami, K., and McCallion, A.S. (2006). Evaluating the biological relevance of putative enhancers using Tol2 transposon-mediated transgenesis in zebrafish. Nat. Protoc. *1*, 1297–1305.
53. Kimmel, C.B., Ballard, W.W., Kimmel, S.R., Ullmann, B., and Schilling, T.F. (1995). Stages of embryonic development of the zebrafish. Dev. Dyn. *203*, 253–310.
54. Whitlock, K.E., and Westerfield, M. (2000). The olfactory placodes of the zebrafish form by convergence of cellular fields at the edge of the neural plate. Development *127*, 3645–3653.
55. Kong, A., Frigge, M.L., Masson, G., Besenbacher, S., Sulem, P., Magnusson, G., Gudjonsson, S.A., Sigurdsson, A., Jonasdottir, A., Jonasdottir, A., et al. (2012). Rate of de novo mutations and the importance of father's age to disease risk. Nature *488*, 471–475.
56. Meynert, A.M., Ansari, M., FitzPatrick, D.R., and Taylor, M.S. (2014). Variant detection sensitivity and biases in whole genome and exome sequencing. BMC Bioinformatics *15*, 247.
57. De Rubeis, S., He, X., Goldberg, A.P., Poultney, C.S., Samocha, K., Cicek, A.E., Kou, Y., Liu, L., Fromer, M., Walker, S., et al.; DDD Study; Homozygosity Mapping Collaborative for Autism; UK10K Consortium (2014). Synaptic, transcriptional and chromatin genes disrupted in autism. Nature *515*, 209–215.
58. de Kok, Y.J., Merkx, G.F., van der Maarel, S.M., Huber, I., Malcolm, S., Ropers, H.H., and Cremers, F.P. (1995). A duplication/paracentric inversion associated with familial X-linked deafness (DFN3) suggests the presence of a regulatory element more than 400 kb upstream of the POU3F4 gene. Hum. Mol. Genet. *4*, 2145–2150.
59. Lin, M., Pedrosa, E., Shah, A., Hrabovsky, A., Maqbool, S., Zheng, D., and Lachman, H.M. (2011). RNA-Seq of human neurons derived from iPS cells reveals candidate long non-coding RNAs involved in neurogenesis and neuropsychiatric disorders. PLoS ONE *6*, e23356.
60. Xu, B., Ionita-Laza, I., Roos, J.L., Boone, B., Woodrick, S., Sun, Y., Levy, S., Gogos, J.A., and Karayiorgou, M. (2012). De novo gene mutations highlight patterns of genetic and neural complexity in schizophrenia. Nat. Genet. *44*, 1365–1369.
61. Jacquemont, S., Coe, B.P., Hersch, M., Duyzend, M.H., Krumm, N., Bergmann, S., Beckmann, J.S., Rosenfeld, J.A., and Eichler, E.E. (2014). A higher mutational burden in females supports a "female protective model" in neurodevelopmental disorders. Am. J. Hum. Genet. *94*, 415–425.
62. Turner, T.N., Sharma, K., Oh, E.C., Liu, Y.P., Collins, R.L., Sosa, M.X., Auer, D.R., Brand, H., Sanders, S.J., Moreno-De-Luca, D., et al. (2015). Loss of δ-catenin function in severe autism. Nature *520*, 51–56.
63. Okuma, T., Honda, R., Ichikawa, G., Tsumagari, N., and Yasuda, H. (1999). In vitro SUMO-1 modification requires two enzymatic steps, E1 and E2. Biochem. Biophys. Res. Commun. *254*, 693–698.
64. Henley, J.M., Craig, T.J., and Wilkinson, K.A. (2014). Neuronal SUMOylation: mechanisms, physiology, and roles in neuronal dysfunction. Physiol. Rev. *94*, 1249–1285.
65. Lionel, A.C., Crosbie, J., Barbosa, N., Goodale, T., Thiruvahindrapuram, B., Rickaby, J., Gazzellone, M., Carson, A.R., Howe, J.L., Wang, Z., et al. (2011). Rare copy number variation discovery and cross-disorder comparisons identify risk genes for ADHD. Sci. Transl. Med. *3*, 95ra75.
66. Prasad, A., Merico, D., Thiruvahindrapuram, B., Wei, J., Lionel, A.C., Sato, D., Rickaby, J., Lu, C., Szatmari, P., Roberts, W., et al. (2012). A discovery resource of rare copy number variations in individuals with autism spectrum disorder. G3 (Bethesda) *2*, 1665–1685.
67. Rivière, J.B., Mirzaa, G.M., O'Roak, B.J., Beddaoui, M., Alcantara, D., Conway, R.L., St-Onge, J., Schwartzentruber, J.A., Gripp, K.W., Nikkel, S.M., et al.; Finding of Rare Disease Genes (FORGE) Canada Consortium (2012). De novo germline and postzygotic mutations in AKT3, PIK3R2 and PIK3CA cause a spectrum of related megalencephaly syndromes. Nat. Genet. *44*, 934–940.
68. Jansen, L.A., Mirzaa, G.M., Ishak, G.E., O'Roak, B.J., Hiatt, J.B., Roden, W.H., Gunter, S.A., Christian, S.L., Collins, S., Adams, C., et al. (2015). PI3K/AKT pathway mutations cause a spectrum of brain malformations from megalencephaly to focal cortical dysplasia. Brain *138*, 1613–1628.
69. Oda, K., Okada, J., Timmerman, L., Rodriguez-Viciana, P., Stokoe, D., Shoji, K., Taketani, Y., Kuramoto, H., Knight, Z.A., Shokat, K.M., and McCormick, F. (2008). PIK3CA cooperates with other phosphatidylinositol 3′-kinase pathway mutations to effect oncogenic transformation. Cancer Res. *68*, 8127–8136.
70. Roche, A.F., Mukherjee, D., Guo, S.M., and Moore, W.M. (1987). Head circumference reference data: birth to 18 years. Pediatrics *79*, 706–712.
71. Qu, Q., Sun, G., Murai, K., Ye, P., Li, W., Asuelime, G., Cheung, Y.T., and Shi, Y. (2013). Wnt7a regulates multiple steps of neurogenesis. Mol. Cell. Biol. *33*, 2551–2559.
72. Bernier, R., Golzio, C., Xiong, B., Stessman, H.A., Coe, B.P., Penn, O., Witherspoon, K., Gerdts, J., Baker, C., Vulto-van Silfhout, A.T., et al. (2014). Disruptive CHD8 mutations define a subtype of autism early in development. Cell *158*, 263–276.
73. Fuerst, P.G., Koizumi, A., Masland, R.H., and Burgess, R.W. (2008). Neurite arborization and mosaic spacing in the mouse retina require DSCAM. Nature *451*, 470–474.
74. de Ligt, J., Willemsen, M.H., van Bon, B.W., Kleefstra, T., Yntema, H.G., Kroes, T., Vulto-van Silfhout, A.T., Koolen, D.A., de Vries, P., Gilissen, C., et al. (2012). Diagnostic exome sequencing in persons with severe intellectual disability. N. Engl. J. Med. *367*, 1921–1929.
75. Girirajan, S., Rosenfeld, J.A., Coe, B.P., Parikh, S., Friedman, N., Goldstein, A., Filipink, R.A., McConnell, J.S., Angle, B., Meschino, W.S., et al. (2012). Phenotypic heterogeneity of genomic disorders and rare copy-number variants. N. Engl. J. Med. *367*, 1321–1331.
76. Girirajan, S., Dennis, M.Y., Baker, C., Malig, M., Coe, B.P., Campbell, C.D., Mark, K., Vu, T.H., Alkan, C., Cheng, Z., et al. (2013). Refinement and discovery of new hotspots of copy-number variation associated with autism spectrum disorder. Am. J. Hum. Genet. *92*, 221–237.
77. Bradshaw, N.J., and Porteous, D.J. (2012). DISC1-binding proteins in neural development, signalling and schizophrenia. Neuropharmacology *62*, 1230–1241.
78. Kilpinen, H., Ylisaukko-Oja, T., Hennah, W., Palo, O.M., Varilo, T., Vanhala, R., Nieminen-von Wendt, T., von Wendt, L., Paunio, T., and Peltonen, L. (2008). Association of DISC1 with autism and Asperger syndrome. Mol. Psychiatry *13*, 187–196.

79. Hodge, J.C., Mitchell, E., Pillalamarri, V., Toler, T.L., Bartel, F., Kearney, H.M., Zou, Y.S., Tan, W.H., Hanscom, C., Kirmani, S., et al. (2014). Disruption of MBD5 contributes to a spectrum of psychopathology and neurodevelopmental abnormalities. Mol. Psychiatry *19*, 368–379.

80. Talkowski, M.E., Mullegama, S.V., Rosenfeld, J.A., van Bon, B.W., Shen, Y., Repnikova, E.A., Gastier-Foster, J., Thrush, D.L., Kathiresan, S., Ruderfer, D.M., et al. (2011). Assessment of 2q23.1 microdeletion syndrome implicates MBD5 as a single causal locus of intellectual disability, epilepsy, and autism spectrum disorder. Am. J. Hum. Genet. *89*, 551–563.

81. Rauch, A., Wieczorek, D., Graf, E., Wieland, T., Endele, S., Schwarzmayr, T., Albrecht, B., Bartholdi, D., Beygo, J., Di Donato, N., et al. (2012). Range of genetic mutations associated with severe non-syndromic sporadic intellectual disability: an exome sequencing study. Lancet *380*, 1674–1682.

82. Fogel, B.L., Wexler, E., Wahnich, A., Friedrich, T., Vijayendran, C., Gao, F., Parikshak, N., Konopka, G., and Geschwind, D.H. (2012). RBFOX1 regulates both splicing and transcriptional networks in human neuronal development. Hum. Mol. Genet. *21*, 4171–4186.

83. Bill, B.R., Lowe, J.K., Dybuncio, C.T., and Fogel, B.L. (2013). Orchestration of neurodevelopmental programs by RBFOX1: implications for autism spectrum disorder. Int. Rev. Neurobiol. *113*, 251–267.

84. Zhao, W.W. (2013). Intragenic deletion of RBFOX1 associated with neurodevelopmental/neuropsychiatric disorders and possibly other clinical presentations. Mol. Cytogenet. *6*, 26.

85. Leff, S.E., Brannan, C.I., Reed, M.L., Ozçelik, T., Francke, U., Copeland, N.G., and Jenkins, N.A. (1992). Maternal imprinting of the mouse Snrpn gene and conserved linkage homology with the human Prader-Willi syndrome region. Nat. Genet. *2*, 259–264.

The American Journal of Human Genetics

Supplemental Data

Genome Sequencing of Autism-Affected Families Reveals Disruption of Putative Noncoding Regulatory DNA

Tychele N. Turner, Fereydoun Hormozdiari, Michael H. Duyzend, Sarah A. McClymont, Paul W. Hook, Ivan Iossifov, Archana Raja, Carl Baker, Kendra Hoekzema, Holly A. Stessman, Michael C. Zody, Bradley J. Nelson, John Huddleston, Richard Sandstrom, Joshua D. Smith, David Hanna, James M. Swanson, Elaine M. Faustman, Michael J. Bamshad, John Stamatoyannopoulos, Deborah A. Nickerson, Andrew S. McCallion, Robert Darnell, and Evan E. Eichler

Supplemental Data

Supplemental Figures

Figure S1: Experimental approach.

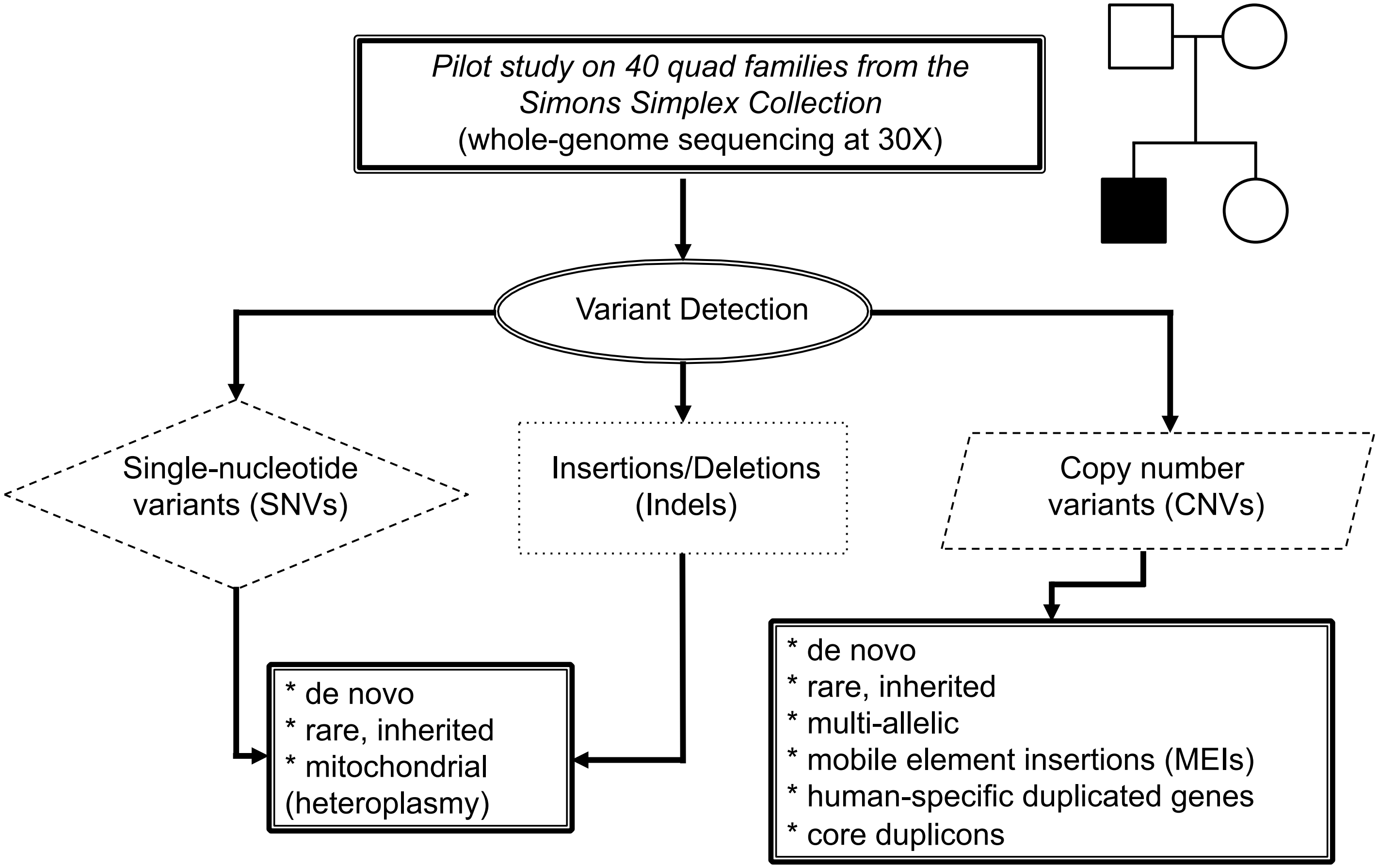
Pilot study on 40 quad families from the Simons Simplex Collection
(whole-genome sequencing at 30X)
Variant Detection
Single-nucleotide variants (SNVs)
Insertions/Deletions (Indels)
Copy number variants (CNVs)
* de novo
* rare, inherited
* mitochondrial (heteroplasmy)
* de novo
* rare, inherited
* multi-allelic
* mobile element insertions (MEIs)
* human-specific duplicated genes
* core duplicons

Figure S1: Flow chart detailing analyses performed on genome data.

Figure S2: Genome sequence properties.

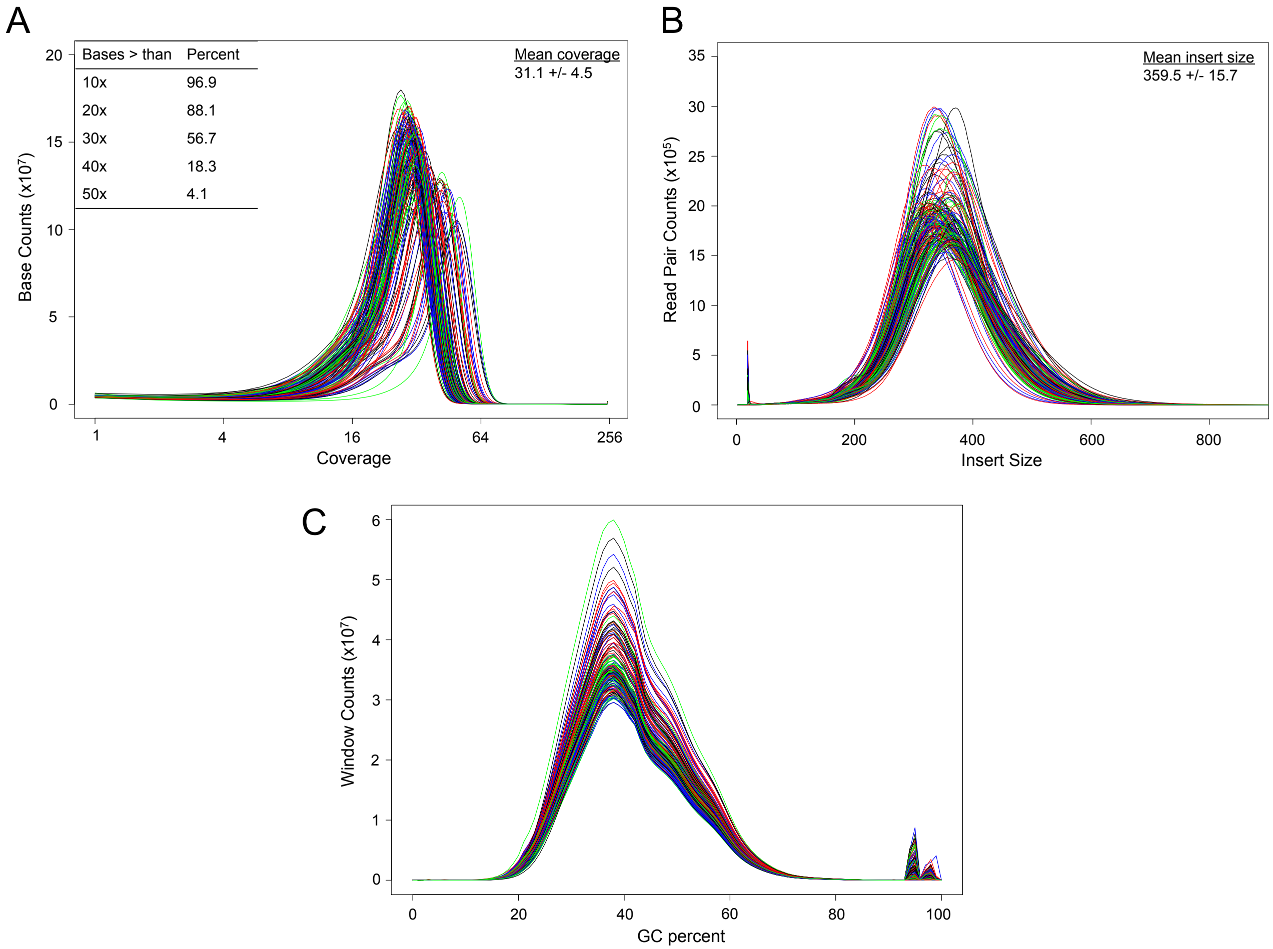

Note: each line represents a unique sample

Figure S2: (A) Coverage of genome sequence data by sample. (B) Insert size metrics. (C) GC percent across genome data.

Figure S3: QC analysis.

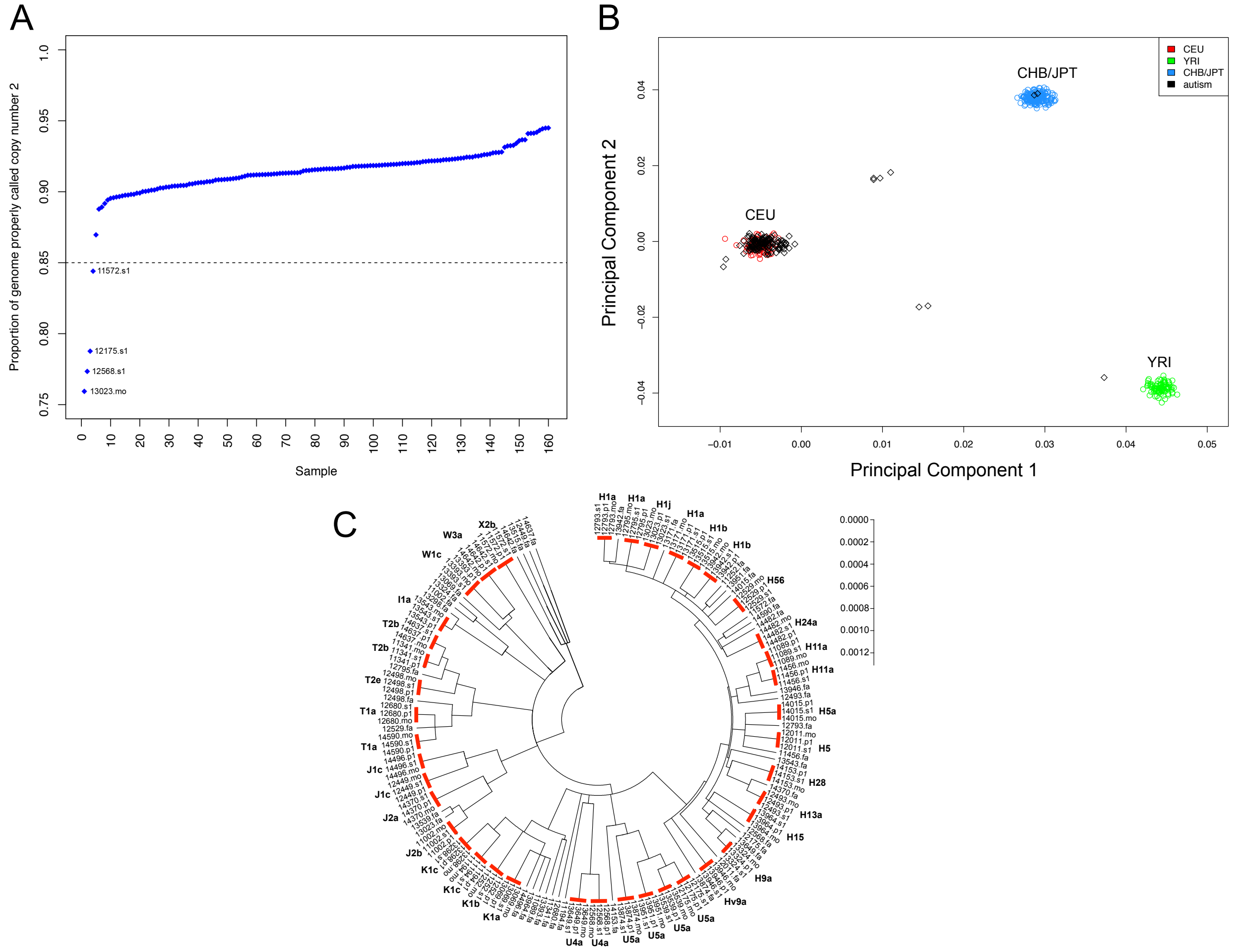

Figure S3: (A) Quality control based on read depth and proper calling of copy number 2 regions. Labeled are samples failing QC. (B) Principal component analysis of SNP data. Shown are three reference populations (CEU: European ancestry, CHB/JPT: Asian ancestry, YRI: African ancestry) and autism samples (shown in black). (C) Neighbor-joining tree of full mitochondrial genomes. Red bars indicate mother, proband, and sibling genomes from a family and haplogroups are labeled as well.

Figure S4: Exome versus genome: concordance.

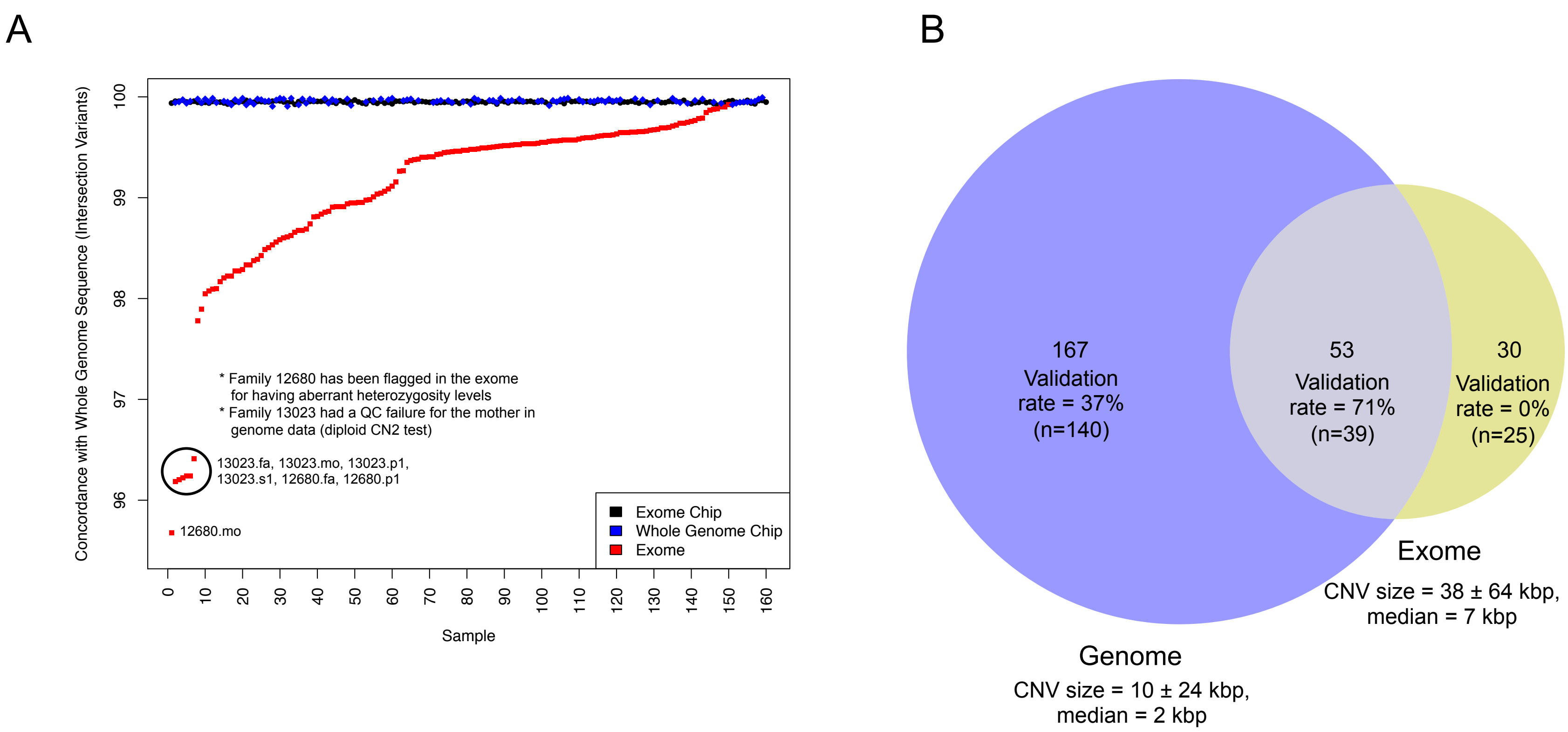

Figure S4: (A) Genotype concordance of genome sequence variants with exome chip, whole-genome chip, and exome data (B) Venn diagram of exome and genome CNV sites within the NimbleGen 36 Mbp exome capture region. Specifically, we compared CNV calls from this study generated by dCGH, GenomeSTRiP, and VariationHunter with calls from exome sequencing analysis [1] made by CoNIFER [2] and XHMM [3]. Calls made by the genome CNV tools are based on read depth, read pair, and split read information while calls made by exome CNV tools are based exclusively on read depth.

Figure S5: Permutation testing to assess clustering of de novo mutations in 100 kbp windows.

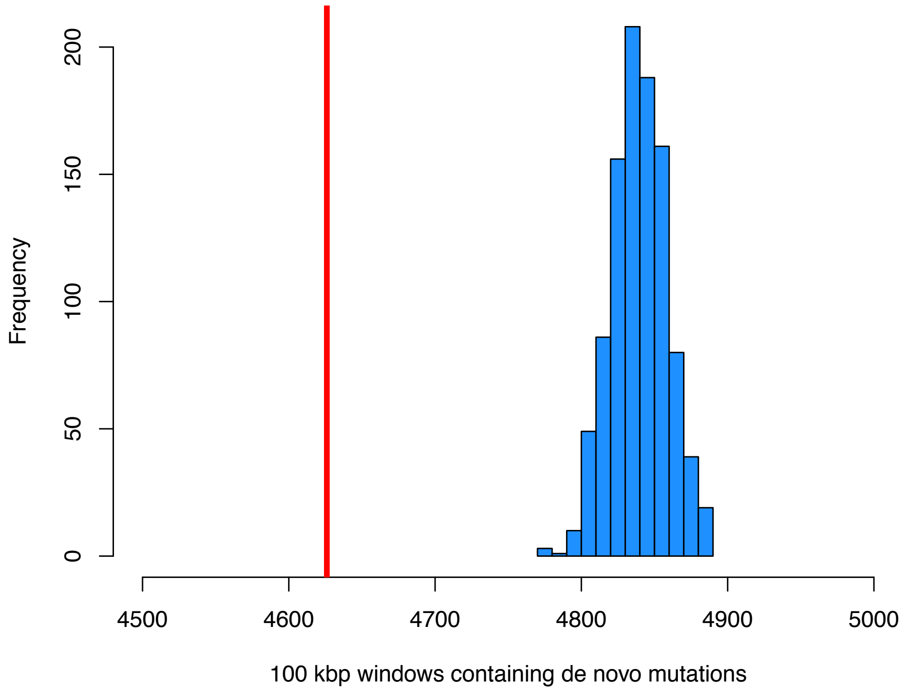

Figure S5: The red line shows the observed number of 100 kbp windows in which de novo mutations from this current study reside. The blue histogram represents the number of windows in which randomly placed de novo mutations reside (1000 permutations shown). The observed number of windows is far less ($p < 1x10^{-3}$) than what is expected if de novo mutations were randomly placed around the genome. The average distance between de novo events was 26.8 ± 31.2 Mbp and there were 189 new mutations where the next nearest de novo mutation within the sample mapped within 1 kbp.

Figure S6: Ranked order of feature importance for de novo variants based on random forest analysis.

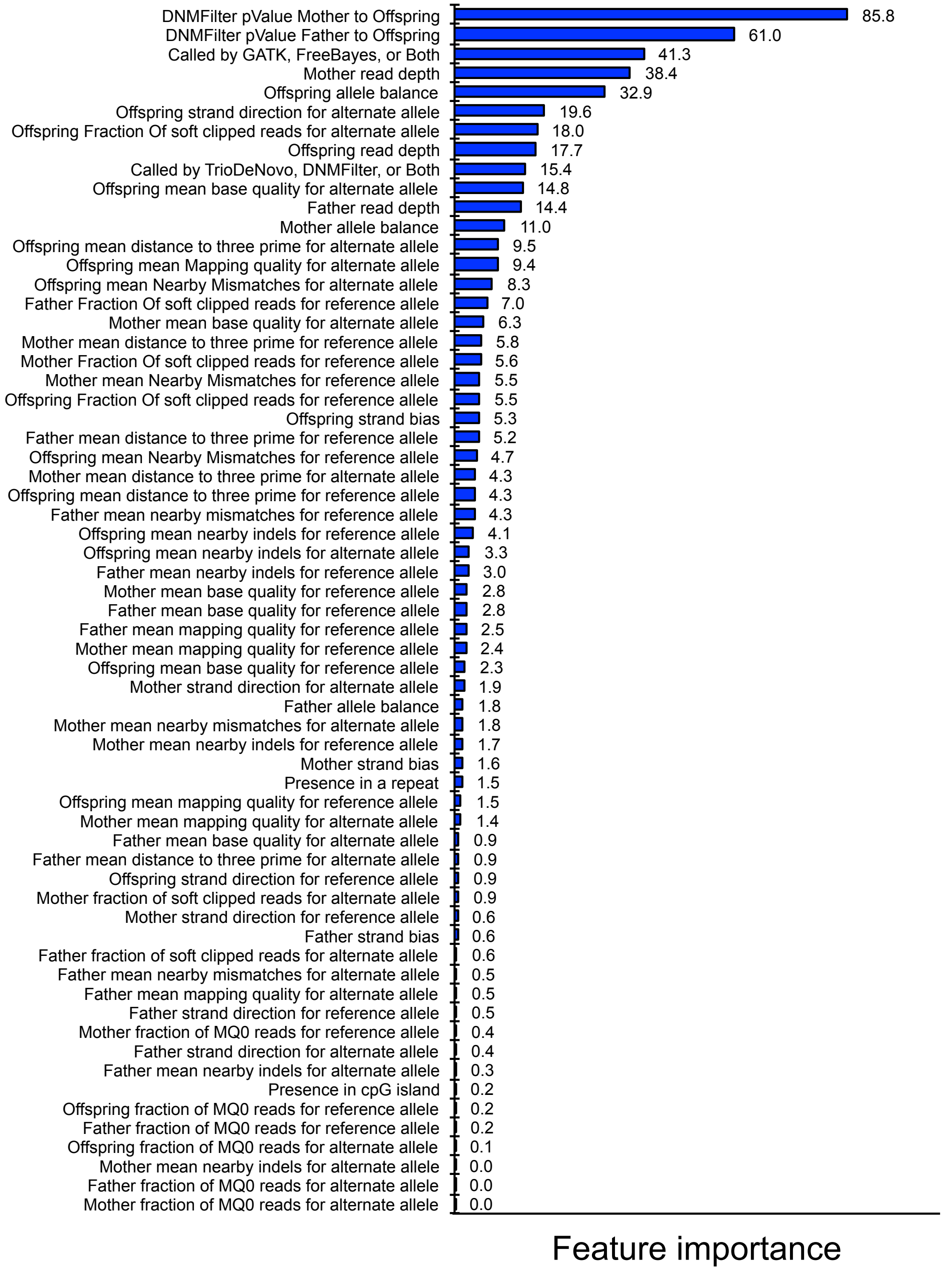

Figure S6: In our assessment of de novo variants we utilized two callers and attempted validation on all exomic and putative regulatory events. We also attempted validation by MIP sequencing on all events in five families. In total, we were able to assess validation status at **1,330** (986 validated and 344 not validated [false positive], validation rate = 74.1%) sites. To determine what may be happening in the ~25% of events that do not validate, we utilized the extract tool in DNMFilter to identify, from the original BAM files, the 59 features used by DNMFilter in its model [4]. In addition we considered four other features: (1) the initial caller (GATK, FreeBayes), (2) if the site maps to a CpG island, (3) if the site is in a repeat, and (4) the type of de novo caller (TrioDeNovo [5], DNMFilter [4]). In total, there were 63 features gathered for each valid / not valid (false positive) site. Using the random forest model, we derived a ranked list of the importance of features.

Figure S7: Distribution of Phred-scaled p-values in events that were validated as de novo (Valid) and those that were not (False positive).

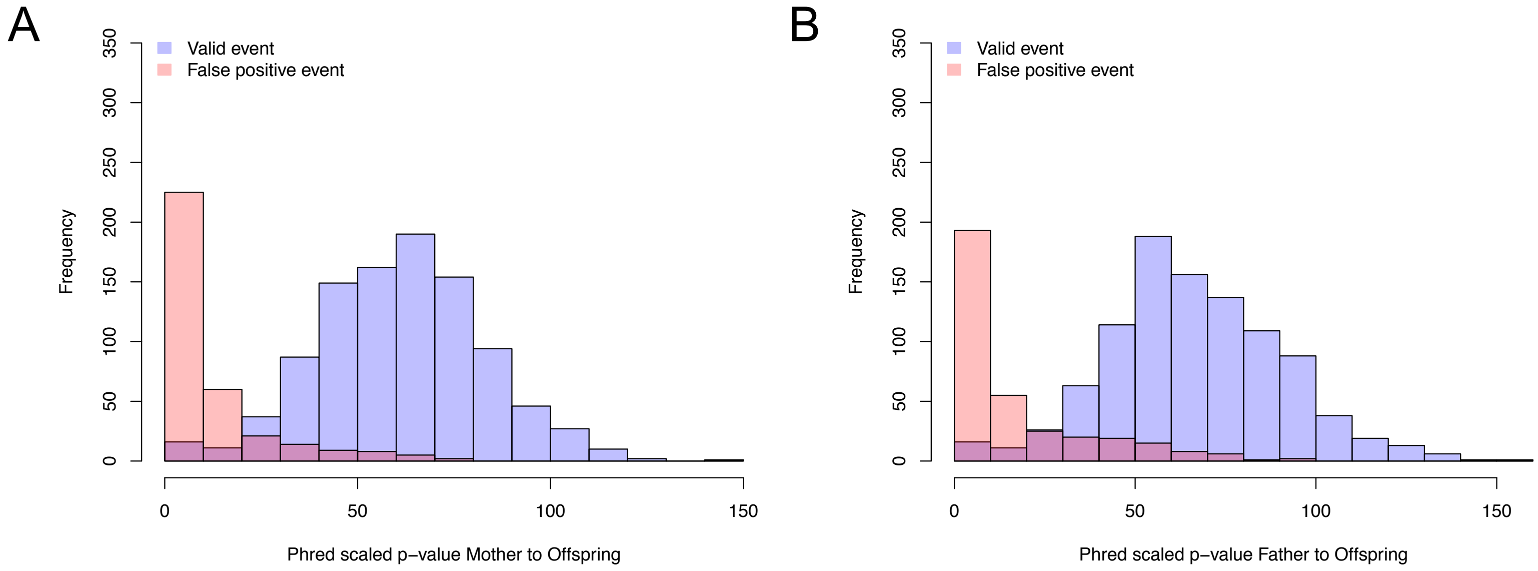

Figure S7: Validated events showed much higher Phred-scaled p-values. The two most important features based on the random forest model for invalidated variants was evidence of inheritance from the mother or father. This is represented as a p-value derived by DNMFilter and is defined in the DNMFilter paper as “the Phred-scaled P-value of a Fisher’s exact test for father/mother and offspring, alt alleles versus ref alleles (two values).” Thus, the most common cause for invalidation was under-calling in one of the parents and a false classification as de novo. This could be easily remedied by considering relative number of alternate allele callers or by considering the DNMFilter p-values. These findings are consistent with the large number of false de novo calls that were found to be inherited during validation.

Figure S8: Counts of variants by initial caller in events that were validated as de novo (Valid) and those that were not (False positive).

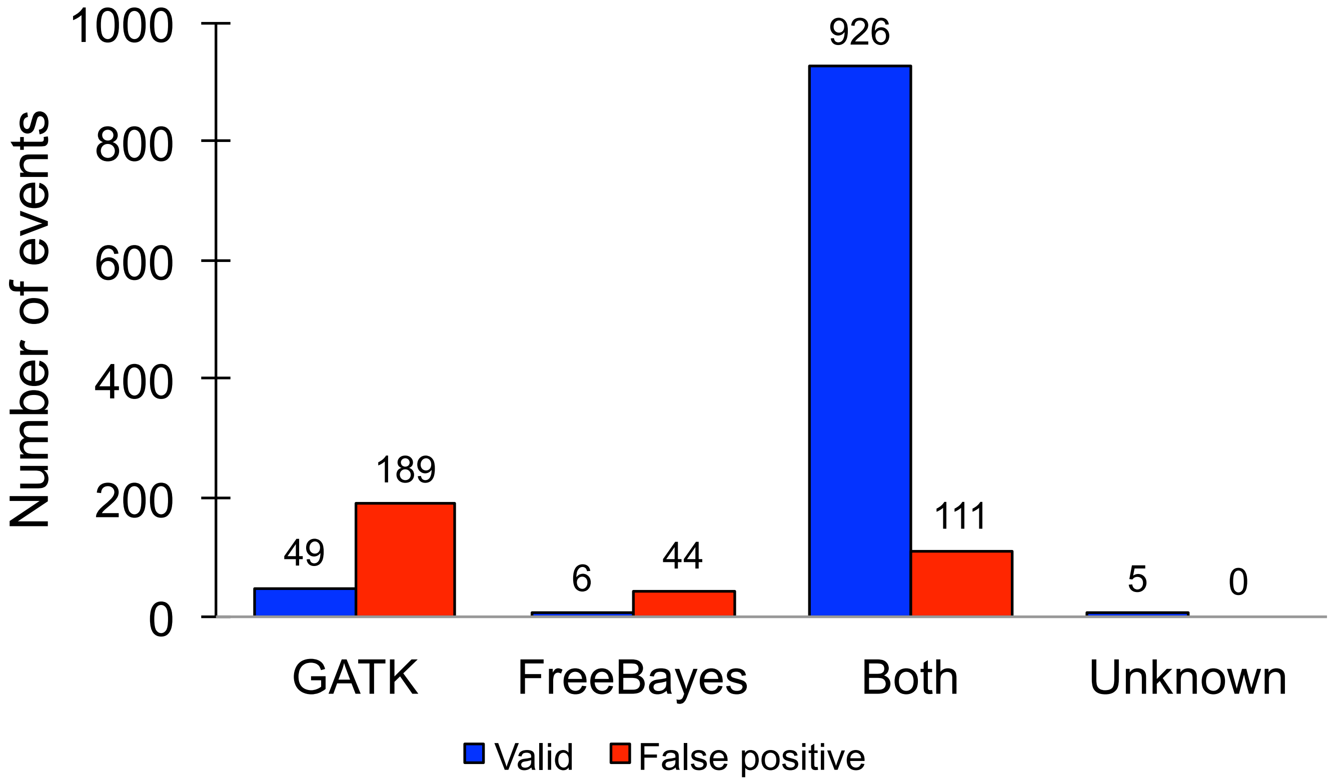

Figure S8: The utility of using both callers increased validation. The type of caller (either GATK or FreeBayes) was identified as another important feature of de novo variant validation. There is, however, higher false positive in either FreeBayes- or GATK-only call sets despite the fact that you recover additional de novo variants. Unknown refers to WES-specific sites.

Figure S9: Additional features important for events that were validated as de novo (Valid) and those that were not (False positive).

Figure S9: Included are (A) mother's read depth at the site; (B) offspring allele balance at the site; (C) offspring mean base quality for alternate allele; (D) offspring read depth; (E) offspring fraction of soft-clipped reads for alternate allele; (F) offspring strand direction at site where 0 indicates all reads are on the same strand and 1 shows presence on both strands; and (G) number of events based on the de novo caller (unknown refers to WES-specific sites).

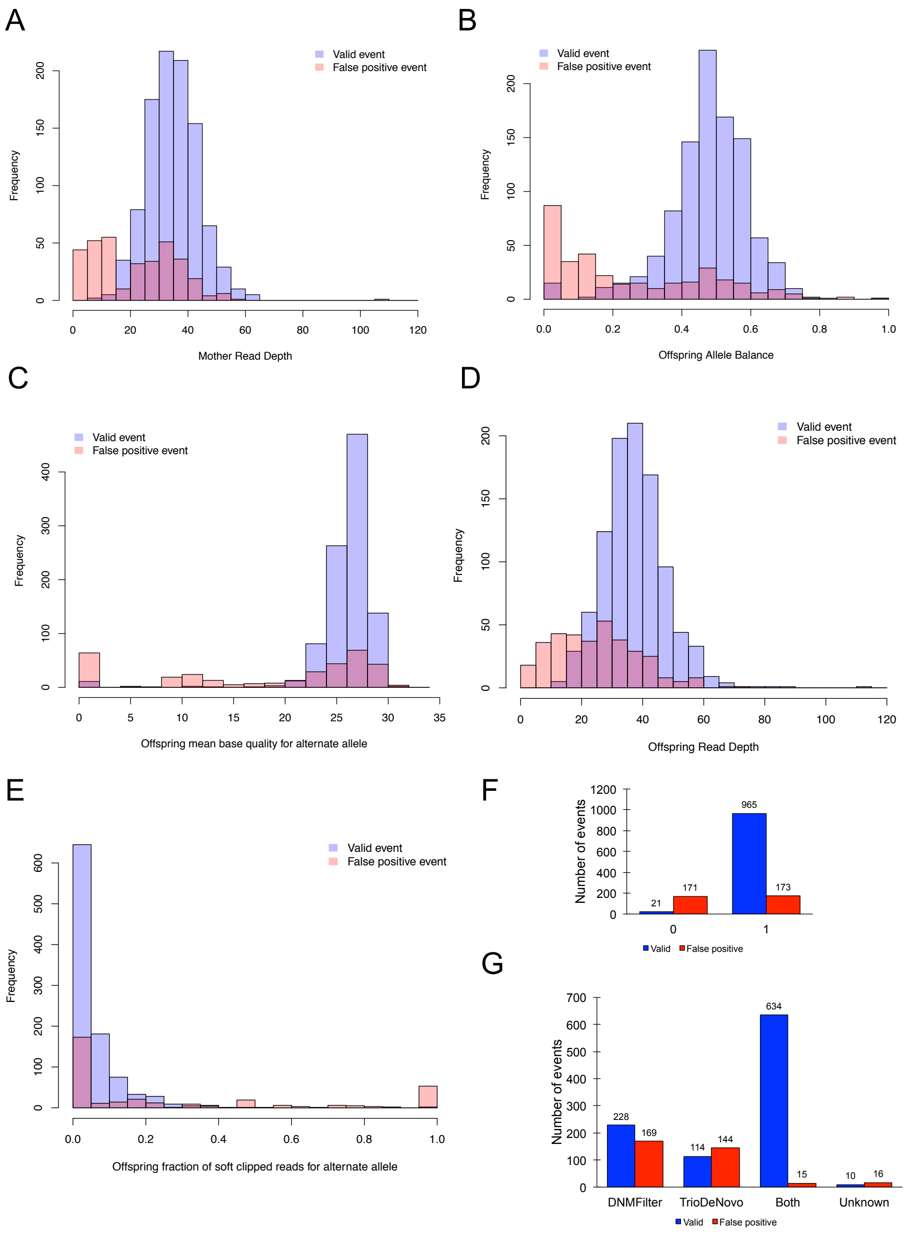

Figure S10: Conditional inference tree for valid de novo and false positive de novo events.

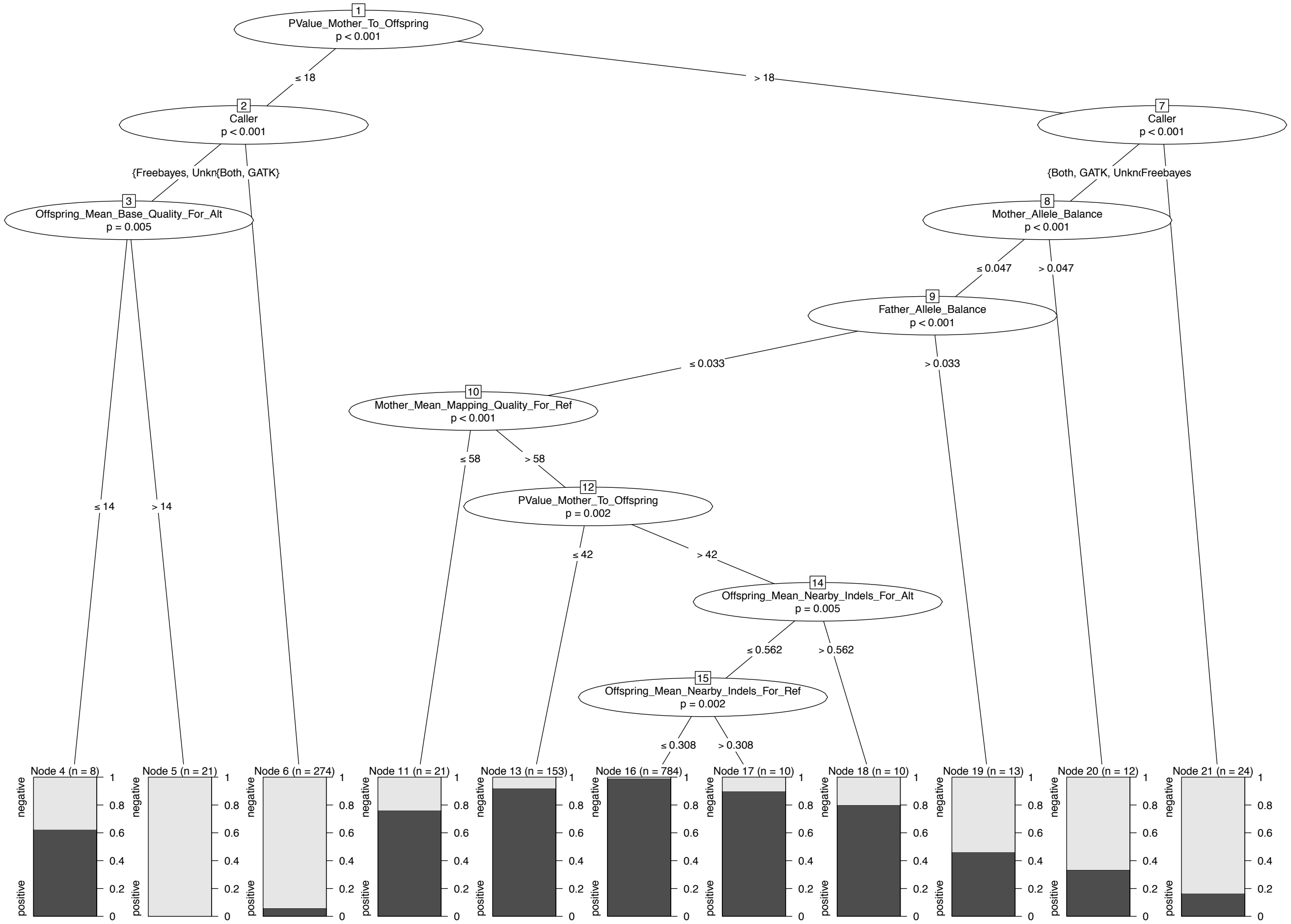

Figure S10: Shown is the best tree generated by the party R package. By following the paths in the tree the number of valid de novo (positive) and not valid de novo (negative) sites can be seen (at the bottom). We were able to generate a conditional inference tree (PARTY [6]) to guide researchers on the precise conditions to maximize discovery of future events. Similar to the random forest method, the tree indicated that the p-value test in the mother and the initial caller were each very critical features in the decision tree. Shown is the entire conditional inference tree and at the bottom is the proportion of validated events (positive) and invalidated events (negative) for each path of the tree. While individual researchers can make their own decision, our results indicate that read depth (Phred >18) and allele balance will discover the maximum set of true variants.

Figure S11: CNV validation.

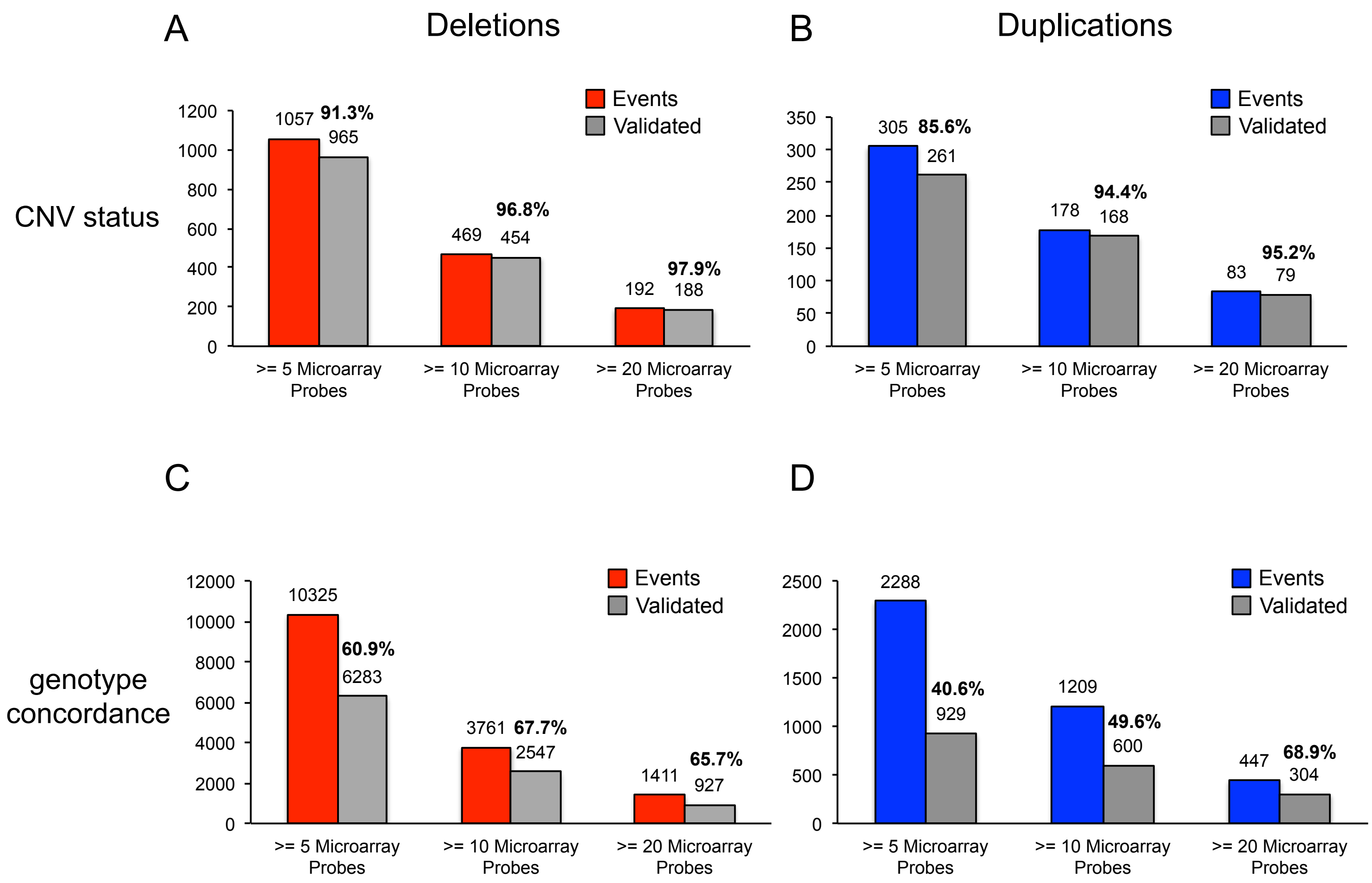

Figure S11: (A) CRLMM validation of deletion sites (B) CRLMM validation of duplication sites (C) Genotype concordance for deletions (D) Genotype concordance for duplications.

Figure S12: Exome versus genome: uniformity analysis.

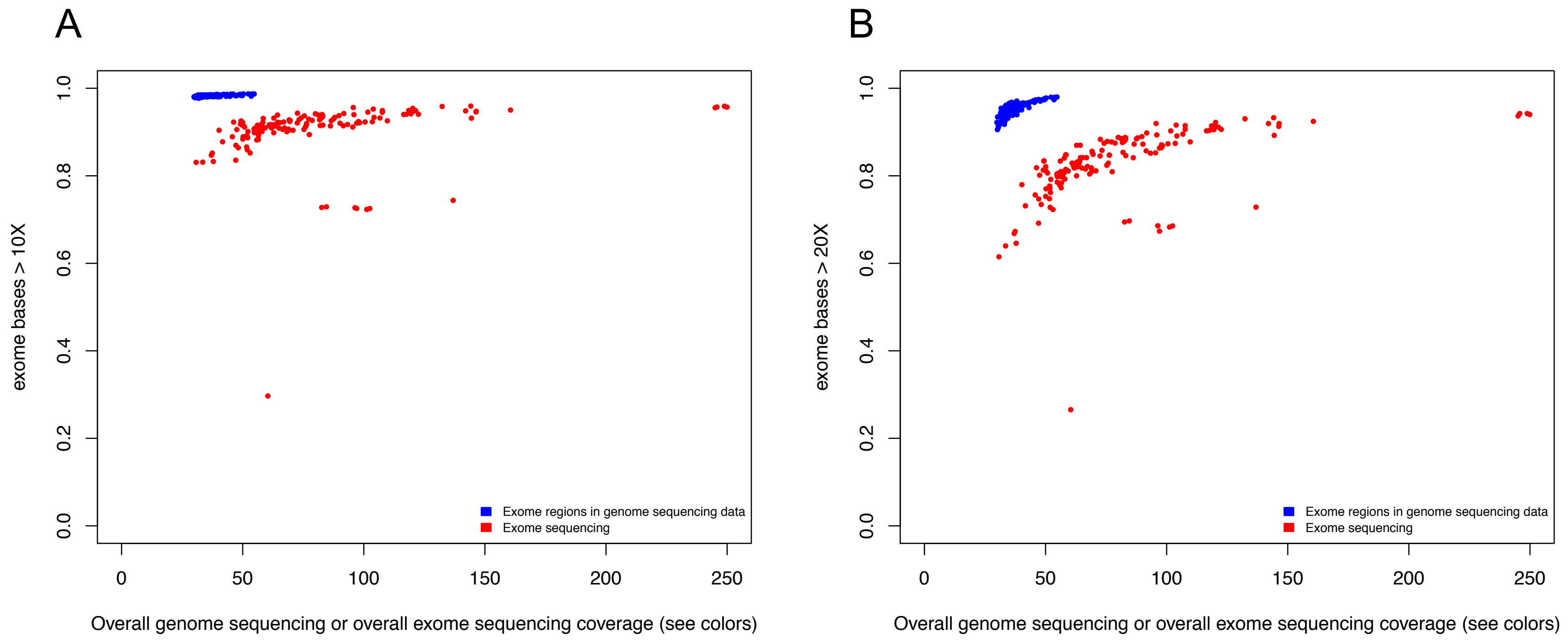

Figure S12: (A) Percent of bases **>10X** in exomic regions from genome sequencing and exome sequencing (B) Percent of bases **>20X** in exomic regions from genome sequencing and exome sequencing. Although WGS showed 36.6 ± 5.4-fold sequence coverage when compared to 81.2 ± 38.6-fold coverage depth by WES, the percent of basepairs with at least 10-fold coverage was greater for WGS (98.3 ± 0.2% vs. 90.4 ± 6.9% for WES) consistent with a more uniform coverage by WGS [7; 8]. As a result, we estimate that an additional 2,126 kbp of exome target was recovered by WGS compared to 42.3 kbp of the exome recovered only by WES.

Figure S13: Genome and exome sequencing identify unique SNV/indel events.

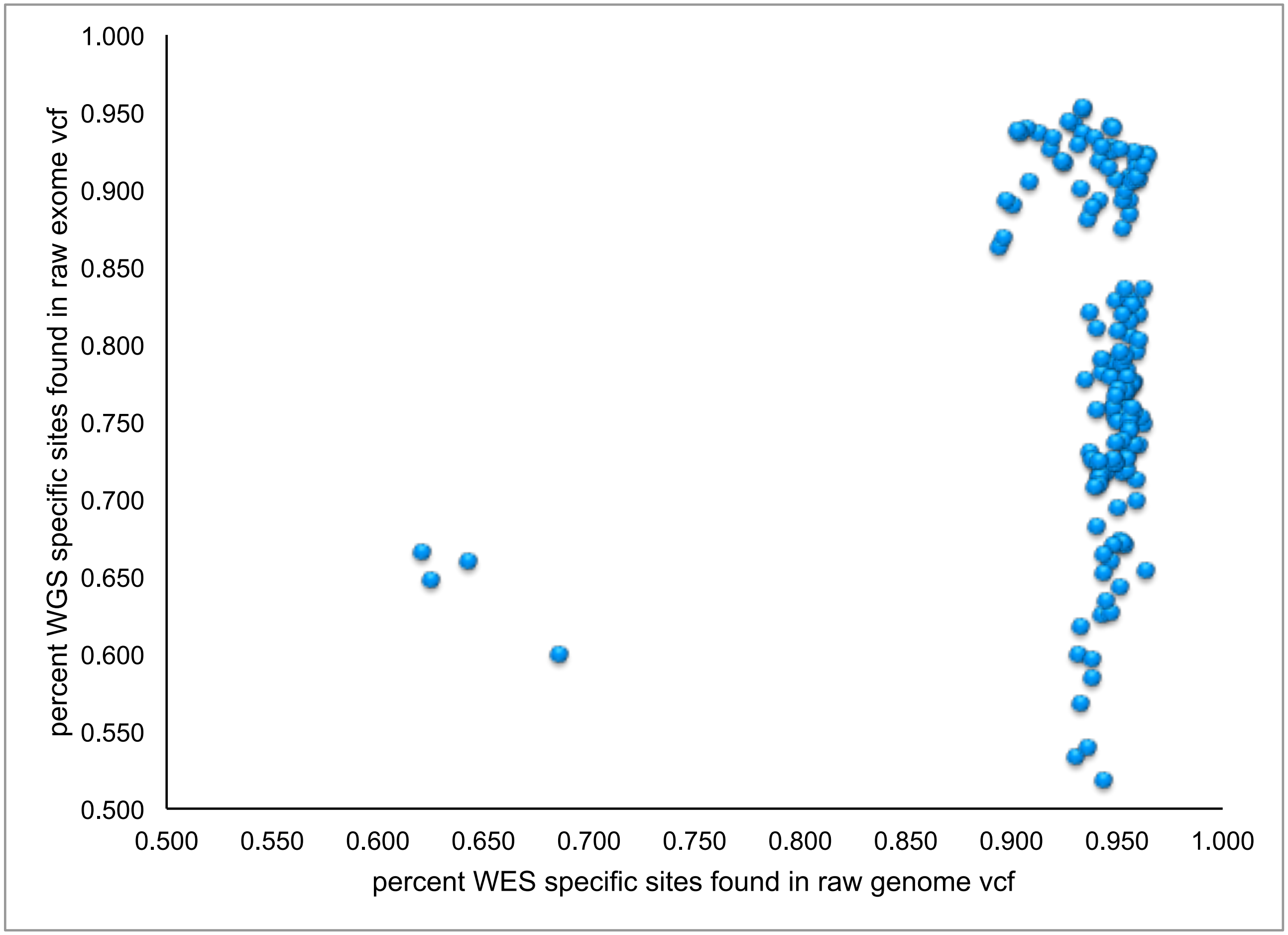

Figure S14: Genome and exome sequencing identify unique CNV events.

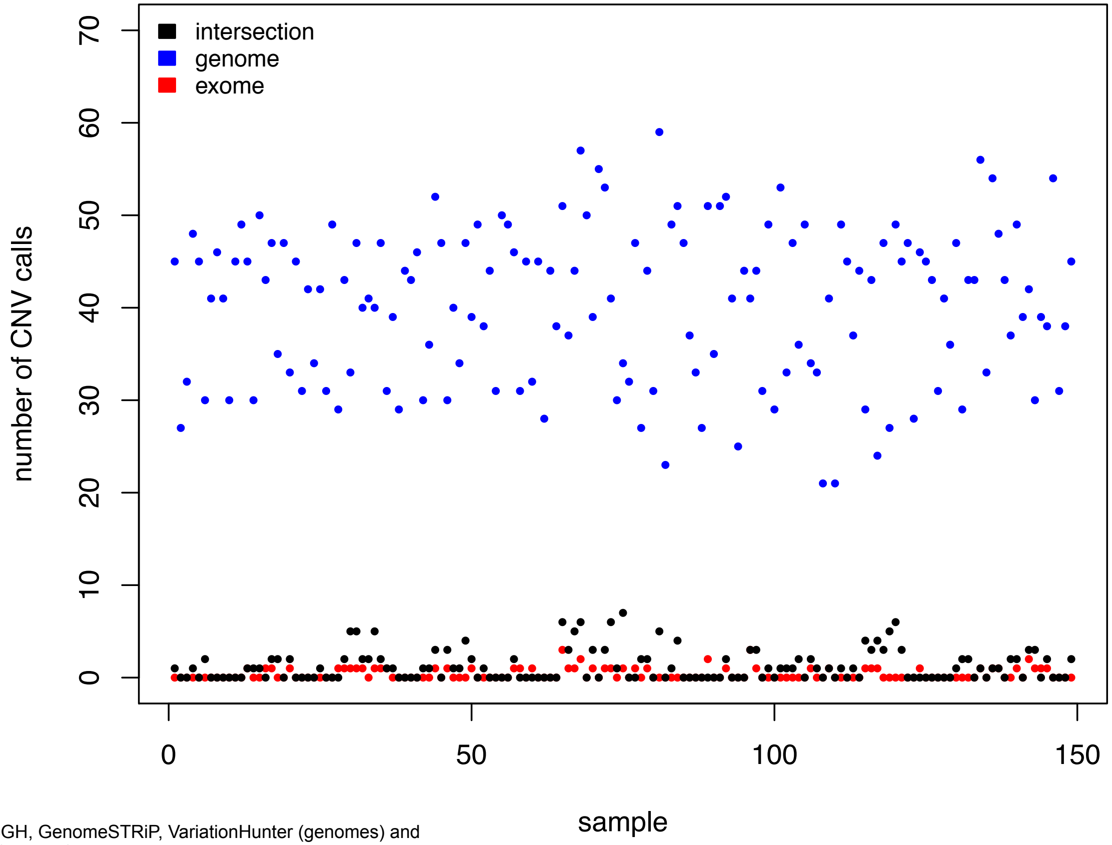

Note: calling by dCGH, GenomeSTRiP, VariationHunter (genomes) and CoNIFER, XHMM (exomes)

Figure S14: Shown are CNVs found in the exome in exome sequencing only, genome sequencing only, and in both exome and genome sequencing. Genome calls were made by dCGH, GenomeSTRiP, and VariationHunter and exome calls by CoNIFER and XHMM. As expected, genome datasets significantly enhance CNV detection. Overall, 167 CNV sites (67%) were called exclusively by WGS, 30 (12%) by WES only, and 53 (21%) by both (Figure S4b) with considerable variability by sampleWe used the SNP microarray validation approach to fairly assess validation rates in each of these sets and found that the intersection had highest validation (validation rate = 71%, n=39), followed by WGS-specific (validation rate = 37%, n=140) and lastly WES-specific events (validation rate = 0% (n=25).

Figure S15: CNV calls detected by WGS and by SNP microarray.

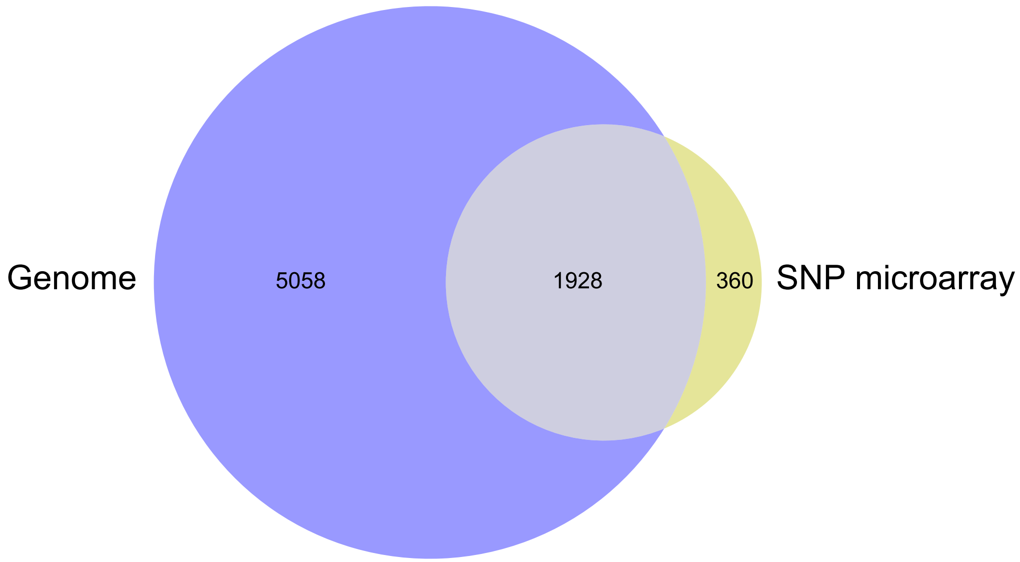

Figure S15: Shown is a Venn diagram of calls identified by one technology or the other and also those detected by both technologies.

Figure S16: Duplications in *SAE1* in autism patients from Lionel et al. 2011, Prasad et al. 2012, and the current study.

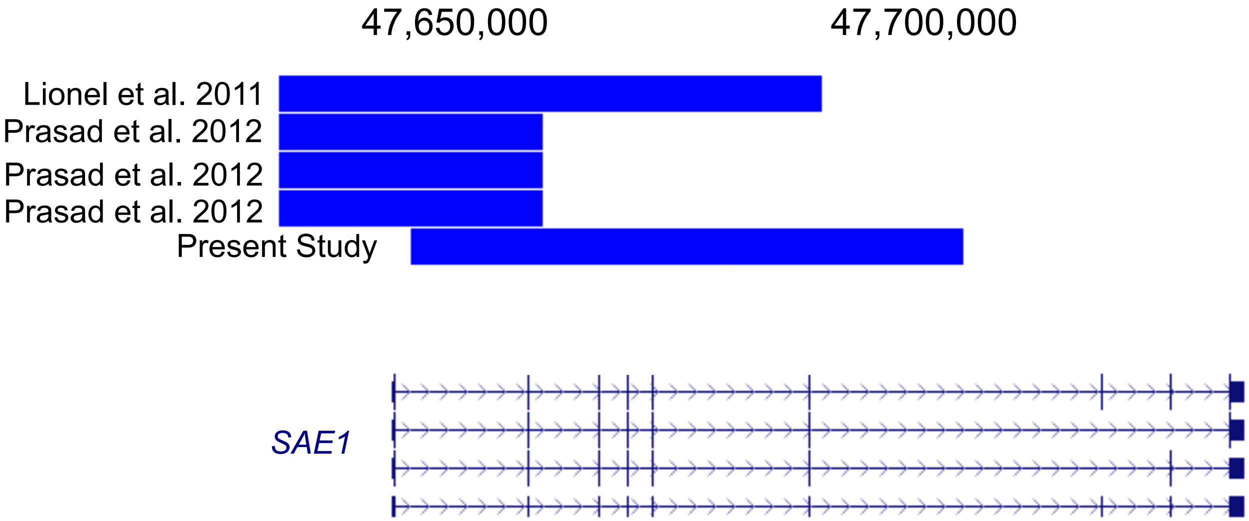

Figure S17: Supplemental images of all other constructs from the functional analysis of CNS DNase I hypersensitivity sites in DSCAM deletion.

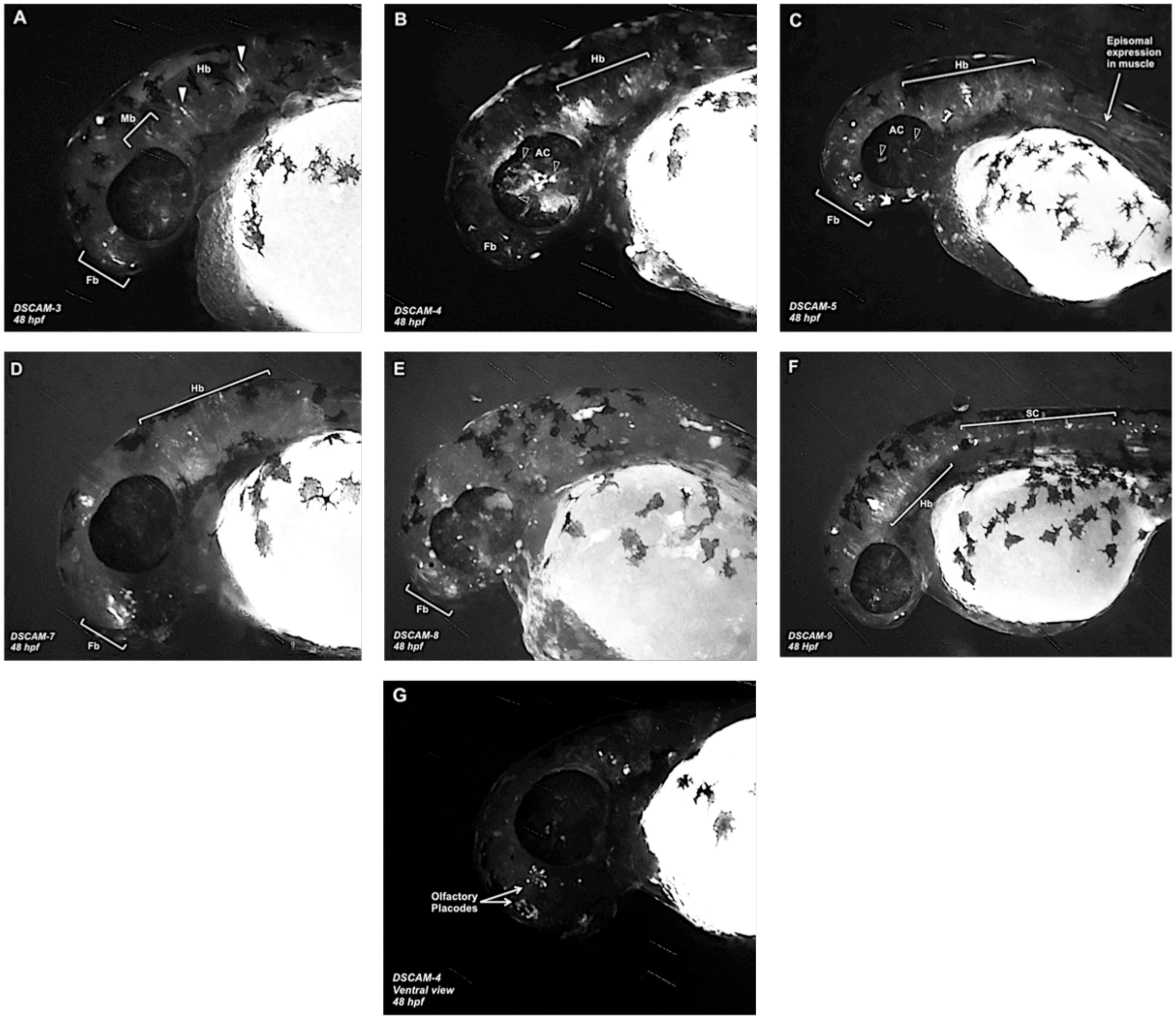

Figure S17: Fb – Forebrain, Mb – Midbrain, Hb – Hindbrain, Am – Amacrine cells, SC – Spinal cord, OP – Olfactory placode

Supplemental References

1. Krumm, N., Turner, T.N., Baker, C., Vives, L., Mohajeri, K., Witherspoon, K., Raja, A., Coe, B.P., Stessman, H.A., He, Z.X., et al. (2015). Excess of rare, inherited truncating mutations in autism. Nature genetics.
2. Krumm, N., Sudmant, P.H., Ko, A., O'Roak, B.J., Malig, M., Coe, B.P., Quinlan, A.R., Nickerson, D.A., and Eichler, E.E. (2012). Copy number variation detection and genotyping from exome sequence data. Genome Res 22, 1525-1532.
3. Fromer, M., Moran, J.L., Chambert, K., Banks, E., Bergen, S.E., Ruderfer, D.M., Handsaker, R.E., McCarroll, S.A., O'Donovan, M.C., Owen, M.J., et al. (2012). Discovery and statistical genotyping of copy-number variation from whole-exome sequencing depth. American journal of human genetics 91, 597-607.
4. Liu, Y., Li, B., Tan, R., Zhu, X., and Wang, Y. (2014). A gradient-boosting approach for filtering de novo mutations in parent-offspring trios. Bioinformatics (Oxford, England) 30, 1830-1836.
5. Wei, Q., Zhan, X., Zhong, X., Liu, Y., Han, Y., Chen, W., and Li, B. (2014). A Bayesian framework for de novo mutation calling in parents-offspring trios. Bioinformatics (Oxford, England).
6. Hothorn, T., Hornik, K., and Zeileis, A. (2006). Unbiased Recursive Partitioning: A Conditional Inference Framework. Journal of Computational and Graphical Statistics 15, 651-674.
7. Meynert, A.M., Ansari, M., FitzPatrick, D.R., and Taylor, M.S. (2014). Variant detection sensitivity and biases in whole genome and exome sequencing. BMC bioinformatics 15, 247.
8. Belkadi, A., Bolze, A., Itan, Y., Cobat, A., Vincent, Q.B., Antipenko, A., Shang, L., Boisson, B., Casanova, J.-L., and Abel, L. (2015). Whole-genome sequencing is more powerful than whole-exome sequencing for detecting exome variants. Proceedings of the National Academy of Sciences.